Final Design Package

EML 4551C – Senior Design – Fall 2011 Deliverable

Unmanned Aircraft System
Team # 14

Ryan Jantzen* Antwon Blackmon* Walker Carr*
Brian Roney# Eric Prast# Alek Hoffman#

[*]Department of Mechanical Engineering, Florida State University, Tallahassee, FL
[#]Department of Electrical and Computer Engineering, Florida State University, Tallahassee, FL

Project Sponsor
Florida Center for Advanced Aero-Propulsion

Project Advisors

Dr. Rajan Kumar, PhD
Department of Mechanical Engineering

Dr. Michael P. Frank, PhD
Department of Electrical and Computer Engineering

Reviewed by Advisor: Dr. Rajan Kumar [ ]
Reviewed by Advisor: Dr. Michael Frank [ ]

Contents

This Page Left Intentionally Blank

1.0 Executive Summary

This report contains the detailed design of the Student Unmanned Aircraft System (SUAS), a product of FAMU/FSU College of Engineering senior design team #14. This UAS was designed in order to compete in the Association for Unmanned Vehicle Systems International (AUVSI) 2012 Student UAS competition, and also to satisfy the requirements of the Mechanical Engineering and Electrical Engineering Capstone project. Our team has been working closely with our main sponsor Florida Center for Advanced Aero-Propulsion (FCAAP), and we have striven to meet the design criteria advised by our primary FCAAP advisor Dr. Rajan Kumar.

The 2012 AUVSI Student UAS competition is based on a fictional military mission. The broad mission of the UAS is to support a team of Navy Seals with intelligence surveillance and intelligence (ISR). The SUAS will complete a mission made up of several separate operations, all of which must be completed within a forty minute time frame. The first operation is the autonomous navigation of the competition course. This operation includes the takeoff and landing phases of flight, waypoint navigation and an area search.

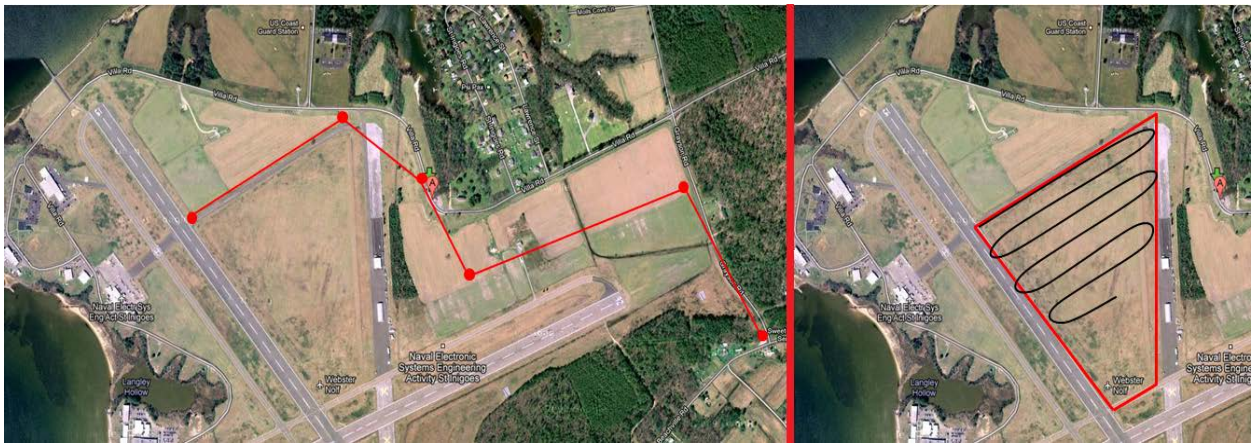

Figure 1.0: Example Waypoint Navigation and Example Area Search Pattern

The second operation is ongoing target identification. The SUAS must be able to identify ground targets with five characteristics: shape, background color, orientation, alphanumeric, and alphanumeric color. The ground targets will be scattered along the competition course, and upon target identification, the image data and target location must be relayed back to the ground station. The third operation is in flight re-tasking, where the flight plan of the UAS is modified by adding additional waypoints or adjusting the search area.

The goal of Team #14 is to design a relatively inexpensive SUAS that is capable of competing in this year's competition by fulfilling these mission requirements while maintaining the safety and integrity of our design and demonstrating the team's proficiency in mechanical, electrical and computer engineering.

2.0 Introduction

An Unmanned Aircraft System (UAS) is an aircraft that operates either by the remote control of a navigator or pilot, or by a completely autonomous avionics system. These aircraft come in a variety of sizes and shapes, and can be designed to complete a wide array of tasks. Because of the availability of relatively cheap UAS software and hardware that is available to the public, there has been a surge in personal UAS design and autonomous aircraft hobby flying. The potential application of the UAS in both the military and civilian sectors has made the design of these aircraft an interesting and important venture.

Currently, the UAS is primarily used in military applications. UASs have been utilized by the military successfully in reconnaissance as well as attack missions. The ability to carry out a mission without placing personnel in combat situations makes using these UAS attractive to our military. The actual use of these aircraft is growing at a rapid pace, with usage in several conflicts abroad and the rising development of small size UASs used by ground infantry. The MQ-9 Reaper hunter killer is an example of a military UAS and is shown in figure 2.

Figure 2.0: The MQ-9 Reaper Hunter Killer UAS

However, as the availability of both UAS software and hardware to the public increased, the civilian sector has begun to utilize the UAS for scientific and research applications. The UAS is a perfect platform for aerial data acquisition. Due to the aircraft's precision and endurance, scientific data can be collected from the sky on a large scale at an affordable budget. The internet has also provided for a large community of UAS hobbyists and designers that share their design information and ideas. This community makes it possible for a hobbyist with little system design experience to purchase and put together a pre-designed UAS. The future of UAS is in the hands of the many aircraft enthusiasts, designers and the professional engineers. The applications of the UAS in the future are unbound.

3.0 Project Management

Senior Design Team #14 consists of six FAMU/FSU engineering students, three Mechanical Engineering majors, two Electrical Engineering majors and one Computer Engineering major. The team is advised by Dr. Rajan Kumar at the Florida Center for Advanced Aero-Propulsion (FCAAP) and Dr. Mike Frank at the FAMU/FSU College of Engineering Electrical and Computer Engineering Department. Dr. Kumar was the primary sponsor advisor and also advised the ME side of the team. Dr. Frank was the ECE side advisor.

3.1 Team Structure

The members of Team #14 were each assigned a team officer position and were further tasked with a particular section of the overall SUAS design. As is seen in figure 3, the aircraft design is broken into 6 sections: Structure, Propulsion, Materials, Power, Controllers and Sensors. Each team member was also responsible for overseeing a specific area of the team organization and performance, determined by their officer position.

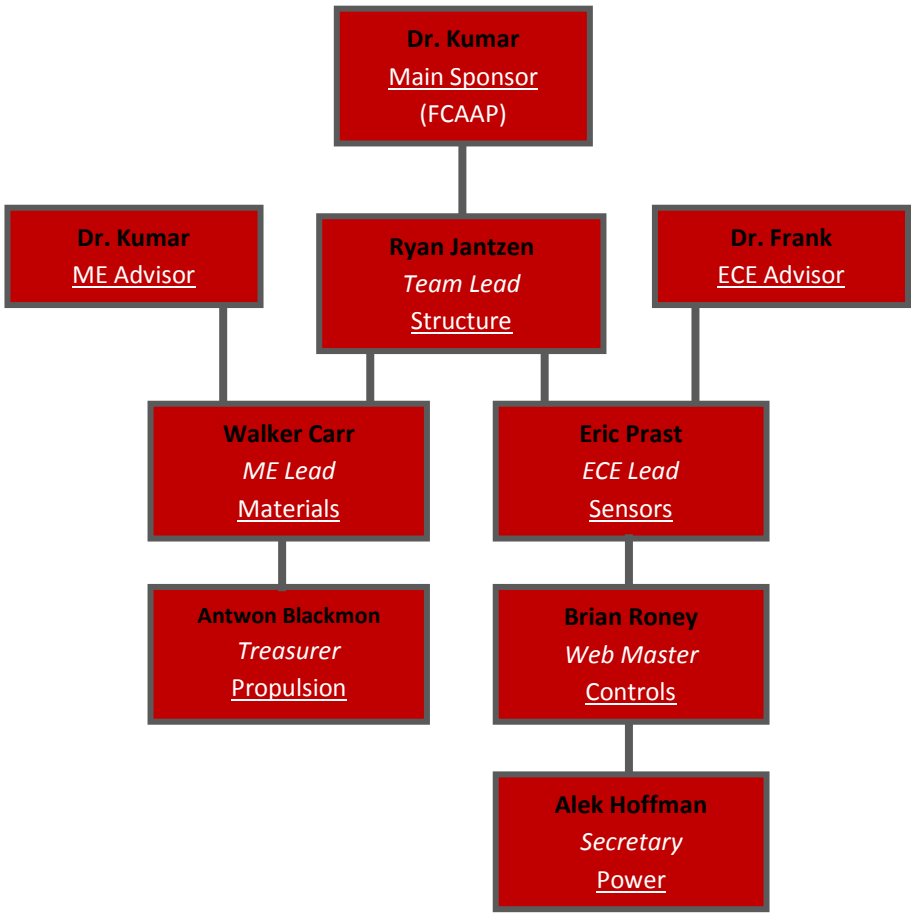

Figure 3.1: Team #14 Organization

The officer descriptions can be found in the Code of Conduct in appendix A. The SUAS design departments were assigned based on experience, interest and engineering major. The structure department covers the design of the aircraft's flight characteristics including the design of all the external parts that make up the aircraft. The materials department deals with the materials used in the construction of the aircraft and also the internal structures of the airframe. The propulsion department is responsible for researching and designing an appropriate propulsion system for the aircraft, including the motor and motor components. The sensors department is responsible for the target recognition and image processing capabilities of the aircraft, including camera design and video transmission. The controls department covers the aircraft's autopilot navigation, all avionics sensors and transmitters, and the human control override. The power department is responsible for designing a power supply system capable of supplying the entire aircraft electronics system with power throughout the entire flight time. One auxiliary section of the project that will need to be designed in the near future is the ground station, where the human/aircraft interface takes place. This aux section will be divided among the ECE students, and will be designed as the aircraft is being built. It is important to note that although the structure of Team # 14 is separated across six persons, all members of the team contribute to the completion of team goals, and in no way is a team member constricted to their assigned departments.

3.2 Time Managament

In order to efficiently design the UAS during the Fall 2011 semester, along with successfully passing all of our engineering courses, time management is of utmost importance. Several tools were utilized by Team # 14 in order to manage our time more effectively. The first tool utilized is the dropbox website. By having an online space accessible by all the members of the team, we are able to collaborate on the completion of team goals, even when we are not physically together. Another tool utilized was Google's calendar program, with which meetings and deadlines were scheduled. By linking the team's individual emails to the calendar, reminders are email out automatically. The final major tool utilized to manage time was the Gannt chart, as shown in figure 3.2.

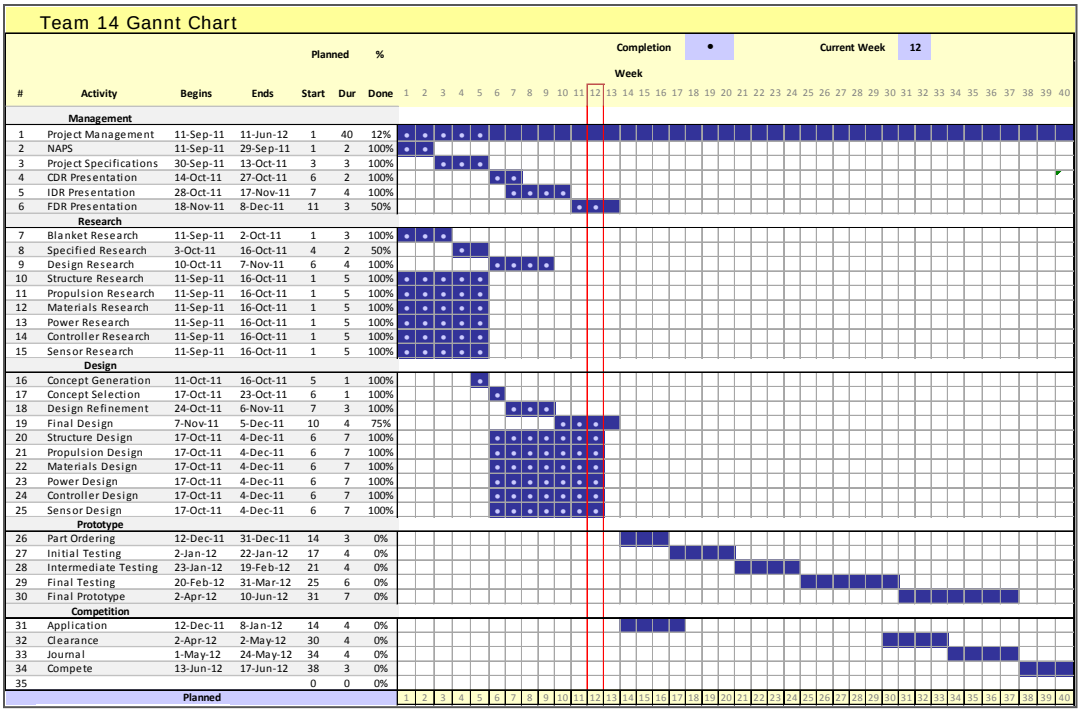

Figure 3.2: Team # 14 Gannt Chart

The Gannt chart visually depicts the project plan which can be broken into five different categories, each with their own number of activities. They are project management, research, design, prototype and competition. Project management deals with the day to day management of the project team, as well as the completion of the required deliverables and presentations. Research covers the overall research into the competition rules, past competitors' designs, and research into the separate components of the design project. The design category contains the four steps of the project design process, as well as the individual design of all the specific components. Prototype deals with physically building the aircraft, testing the aircraft and preparing for the competition. The competition category contains the final steps of the design project goal, which are the requirements of entry into the competition, as well as the completion of the actual competition. A full size Gannt chart is included in Appendix A

4.0 Aircraft Design

4.1 Constraint Analysis

We started the sizing process of our aircraft by doing a constraint analysis for the power loading (P/W) and wing loading (W/S) that would be required to meet all of the design requirements of our aircraft. Power loading is the power required for our aircraft normalized by the weight of the aircraft while wing loading is the weight of the aircraft normalized by the wing area. The constraint analysis takes into consideration all the flight design requirements, such as stall, cruise, takeoff and landing requirements, and helps determine a "design" point where all these requirements are met. Equations for each of these flight design requirements were given by Raymer (2006) that were derived using equations of motion as well as relationships for the specific flight requirement to get it in terms of power loading and wing loading.

From this constraint diagram, we determined an initial power loading of 14.25 Watts/lb and an initial wing loading of 2.71 lb/in^2.

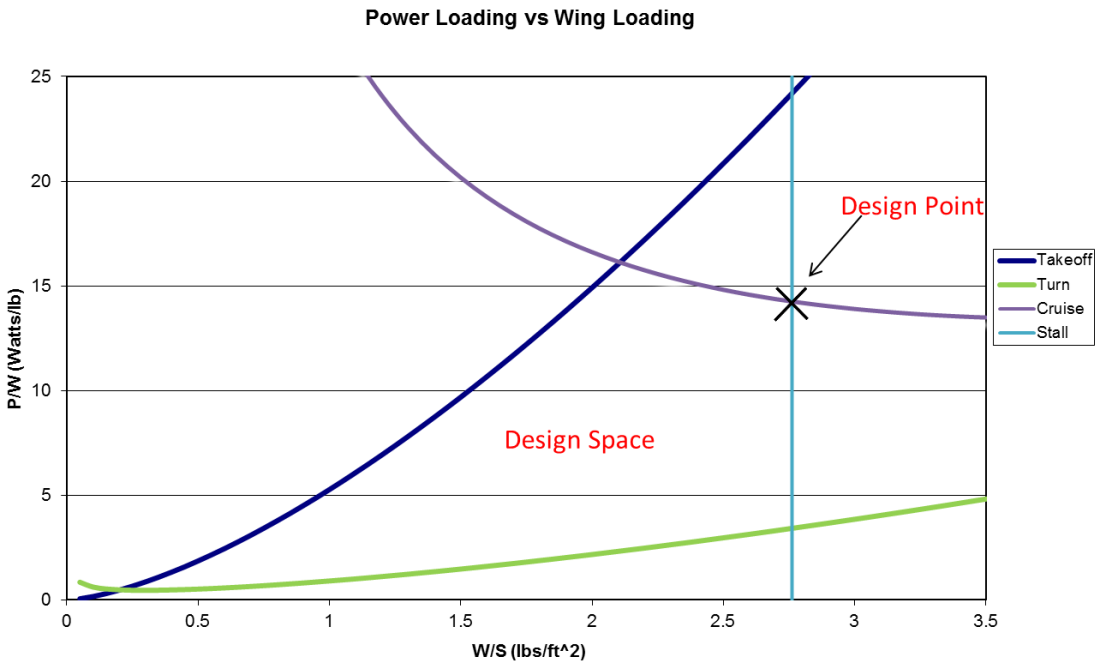

Figure 4.1: Constraint diagram used for the initial power loading and wing loading.

4.2 Wing Design and Analysis:

The next decision that must be made is the configuration of the wing for our aerial vehicle. When designing the wings, performance, stability, manufacturability, operational requirements and flight safety must all be taken into account. The wings must provide sufficient lift to the aircraft during all phases of flight while minimizing the drag.

Airfoil Selection:

The first decision we made during the design of our wings was the selection of our airfoil. The airfoil used for our design must be adequate for all phases of our mission profile. Since we are designing a smaller UAV that will be traveling at lower speeds, we expect that the Reynolds number for our design to be relatively low compared to the Reynolds number seen on commercial or military aircraft. There are many different airfoils that are designed specifically for aircraft flying at a low Reynolds number. Some of the low Reynolds number airfoils that we investigated include the SD 7037, the SD 7032, the NACA 4412, and the NACA 4415, which are shown in figure 2.

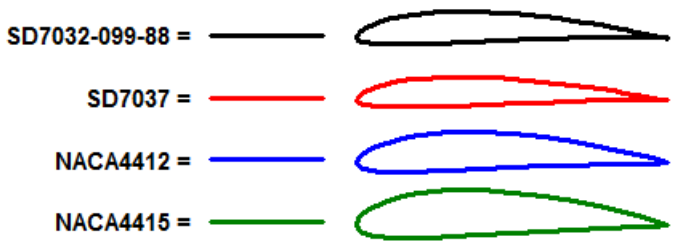

Figure 4.2: Airfoils investigated for our design

For the selection of the airfoil for our design, we decided to look for an airfoil that possesses a high coefficient of lift while keeping the drag to a minimum. Due to the design requirements of having to loiter and take aerial photography, we foresee having to fly at lower speeds while imaging targets on the ground. This requires that the airfoil that is selected must have a gradual stall at lower speeds and higher angle of attack. The following figures compare the lift curves, drag curves, and drag polars produced from a wing design program called Profili, which uses the well-known X-FOIL program to solve for the airfoil polars.

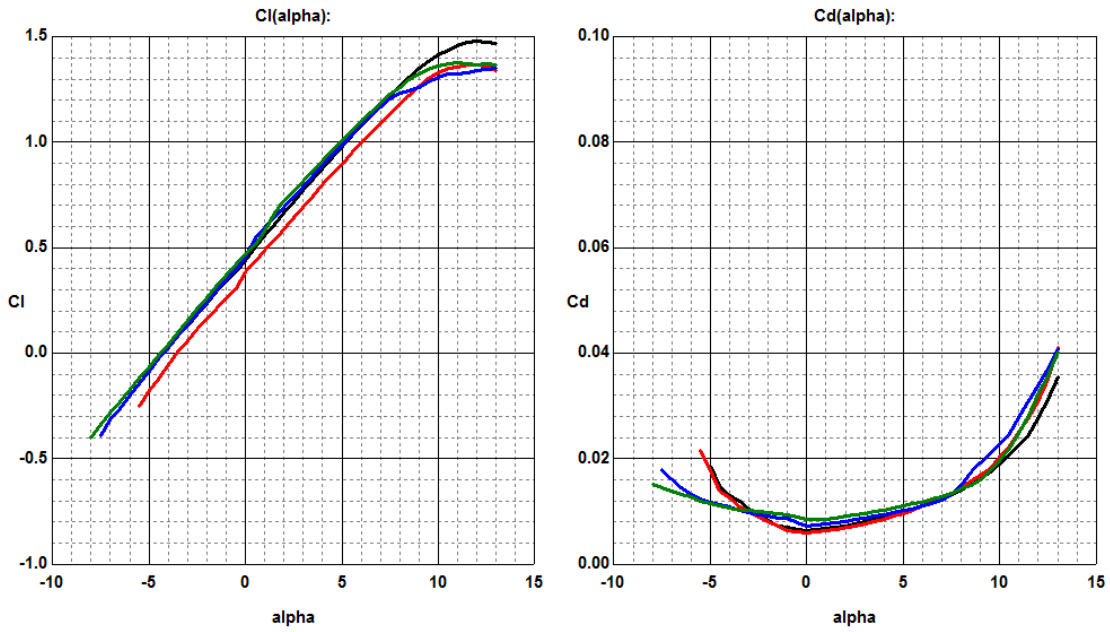

Figure 4.3: Lift and drag curves for aprx. Reynolds number of 400,000.

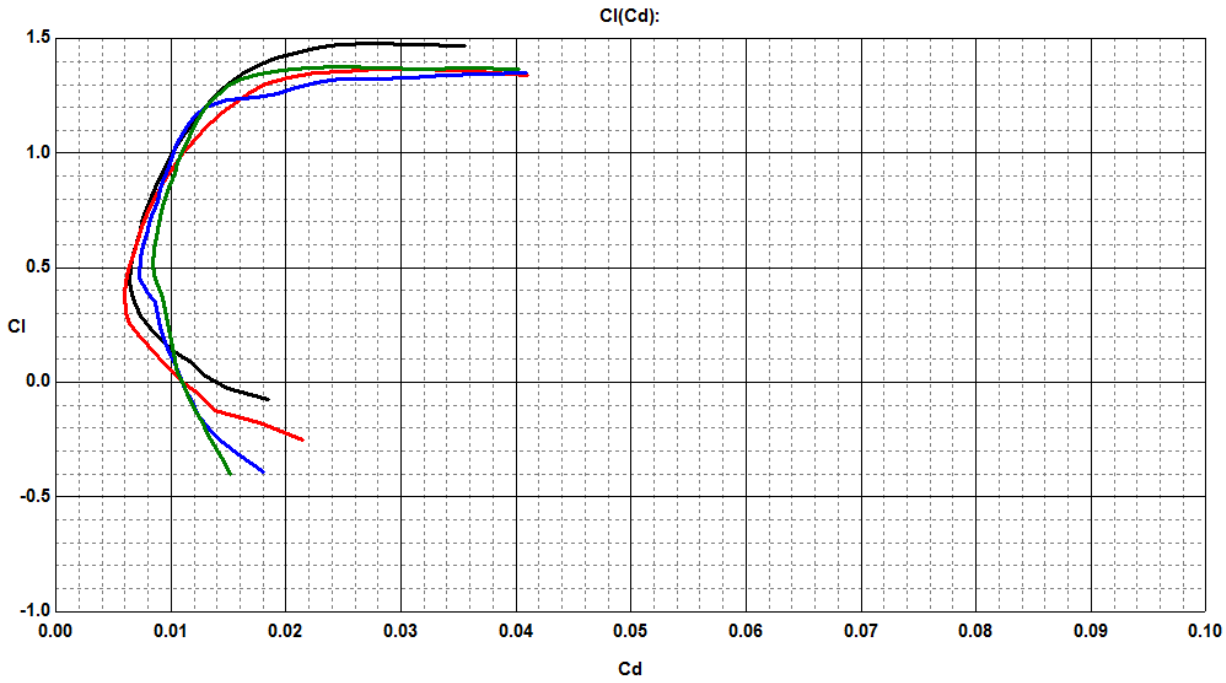

Figure 4.4: Drag polar for an approximate operating Reynolds number of 400,000.

By comparing the following lift and drag curves and drag polars, it seems that the SD 7032 is the clear winner for having the highest and lowest drag. Unfortunately, we decided that this airfoil would not be adequate for our design because of how thin it is. This would not only be hard to manufacture but also it would be structurally weaker than the thicker designs due to its relatively small thickness. The airfoil we found to best fit our mission profile was the NACA 4412. We chose this airfoil mainly due to the gradual stall that it occurs when operating at higher angles of attack. As mentioned previously, we foresee ourselves operating at lower stalling speeds while loitering and taking aerial photography so having a gradual stall that is easily recoverable was a major decision factor. The NACA 4412 airfoil and its major operating parameters are shown in figure 5.

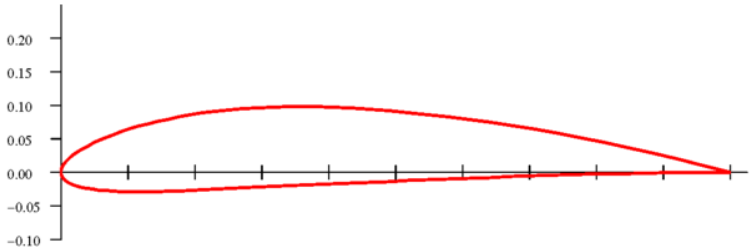

NACA 4412	
Max CL	1.51
Max CL angle	11.00
Max L/D	57.20
Max L/D angle	5.50
Max L/D CL	1.19
Stall angle	6.00
Zero-lift angle	-4.00

Figure 4.5: The NACA 4412 airfoil and its operating parameters.

Planform Design:

After selecting the airfoil for our design, we then began designing the wing planform for our UAV. We first determined the wing area for our design from the previous constraint analysis that was conducted and the initial weight that was determined based on existing aircraft. For a gross take-off weight of 18lbs and the determined wing loading of 2.72 lb/ft^2, we determined our initial wing area to be 6.62 ft^2. After determining the area of the wing, we were able to start selecting how the geometry of our wing would be laid out. This was done with the help of well-known aircraft design books, such as Daniel Raymer's Aircraft Design: A Conceptual Approach (2006). This book has an immense amount of suggestions for optimal aircraft design as well as statistical data from known aircraft.

The two main geometric features that we were concerned with in the initial design of our wing planform were the aspect and taper ratios. The aspect ratio is the ratio of the span of the wing to the chord of the wing. We have decided on using an aspect ratio of 10 for the design of our UAV because higher aspect ratios tend to lead to high aerodynamic efficiency (L/D).

The taper ratio is the ratio of the tip chord length to the root chord length. Wings that are tapered effect the lift distribution along the span of the wing, making it more elliptical which is the most efficient wing planform for the design of an aircraft. Since elliptic wings are expensive and difficult to manufacture, we plan on implementing a tapered wing into the design of our wing. The have chosen to use a taper ratio of 0.45 based on the recommendation given by Raymer (2006) who says it produces a lift distribution that is very close to the ideal elliptical distribution.

4.3 Empennage Design and Analysis

Airfoil Selection:

When designing an empennage of an aircraft, stability, trim and control characteristics must be kept in mind. One of the main objectives for the tail of an aircraft is to keep the aircraft stable in all phases of flight. We used the same methodologies of the previous wing design section for the design of the empennage of our aircraft. The first decision we made when designing the tail of our aircraft was the airfoil it would use. We selected the NACA 0012 symmetric airfoil for both the vertical and horizontal tail geometries. We selected a symmetric airfoil for our tail because they are known to provide stability against pitching moments when used for the horizontal tail and they provide stability against yawing moments when used for the vertical tail. Figure 6 shows the NACA 0012 geometry and lists it main flight parameters.

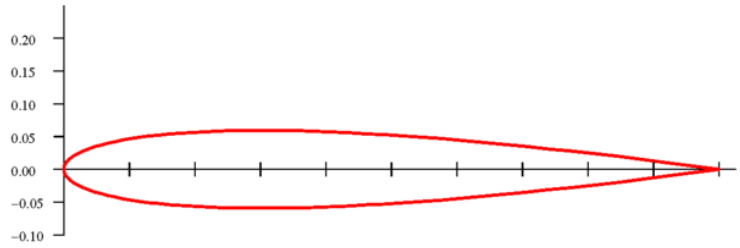

NACA 0012	
Max CL	1.51
Max CL angle	11
Max L/D	57.2
Max L/D angle	5.5
Max L/D CL	1.19
Stall angle	6
Zero-lift angle	-4

Figure 4.6: NACA 0012 airfoil that will be used for the horizontal and vertical tails.

Tail Volume and Moment Arm:

For an aircraft with a front-mounted engine, Raymer (2006) suggests the tail arm to be about 60% of the fuselage length. The lever arms of the horizontal (L_{HT}) and vertical (L_{VT}) stabilizers are the distance between the quarter chord points of the mean aerodynamic chords (MAC) of the surfaces and the quarter chord point of the MAC of the main wing. By finding the moment arms for the horizontal and vertical tails, we were able to use the equations below, given by Raymer (2006), to determine the horizontal and vertical tail areas.

$$S_{HT} = \frac{c_{HT} b_w S_w}{L_{HT}}$$

$$S_{VT} = \frac{c_{VT} b_w S_w}{L_{VT}}$$

Here, c_{HT} and c_{VT} are the horizontal and vertical tail volume coefficients, respectively. These coefficients are based on empirical data and are given to be 0.7 for the horizontal tail and 0.04 for the vertical tail.

XFLR5 Analysis:

After determining the main geometric and aerodynamic features of our wing and tail, we used an analysis program called XFLR5 to determine the performance of our initial layout. This program lets you design the wings and tails of aircraft operating at low Reynolds numbers. The first analysis we performed was the aircraft operating at cruise conditions to determine the lift, drag and pitching moment coefficients in a stable flight regime. The output of the analysis is shown in figure 7. This figure shows the span-wise distribution of lift over the wing of the aircraft, the induced drag profile and the downwash produced by the wing and tail. This also shows the streamlines over the wing along with the tip vorticies produced as a result of the difference of pressure at the tips of the wings.

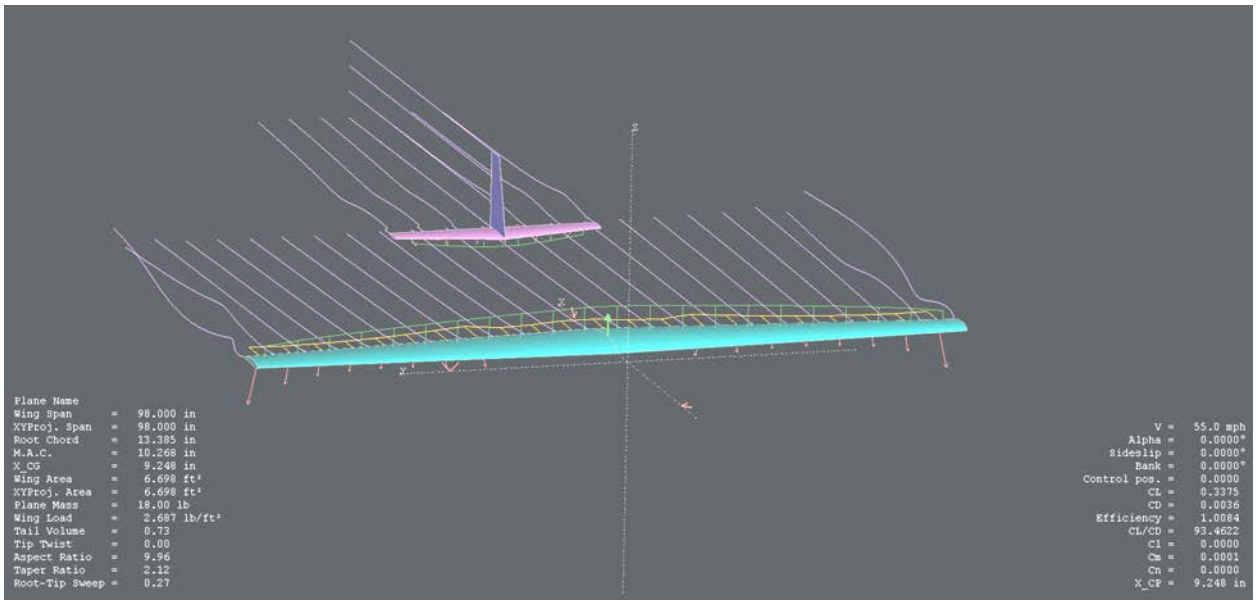

Figure 4.7: XFLR5 Output for Cruise Conditions (55 mph)

This program allows you to run cases at multiple angles of attack to determine the lift, pitching moment, aerodynamic efficiency and drag polars as a function of the angle of attack for the aircraft configuration. These are shown in figure 8. Starting from the top left, the drag polar shows that as the angle of attack is increased, the coefficient of lift is increased and as a result the coefficient of drag is increased as well. The plot on the top right shows the coefficient of lift increases linearly for the three dimensional wing as the angle of attack is increased. The plot below this (bottom right) shows an approximation of the aerodynamic efficiency. It is shown that as the angle of attack is increased from a negative angle to a more positive one, the aerodynamic efficiency is decreased. This is to be expected because as lift is increased, the drag is increased as well. The figure on the bottom left shows the coefficient of pitching moment as a function of the angle of attack. It can be seen that as the angle of attack is increased, i.e. the plane is pitching up; there is a negative moment that resists the upward pitch. This plot also shows that at a zero degree angle of attack, there is no pitching moment about the aircraft. This is due to the fact that the center of pressure at a zero degree angle of attack coincides with the center of gravity. This shows that the configuration has initial stabilizing effects when disturbed from equilibrium. A more detailed stability analysis is currently under way to determine how the aircraft reacts to disturbances as well as deflections of the control surfaces.

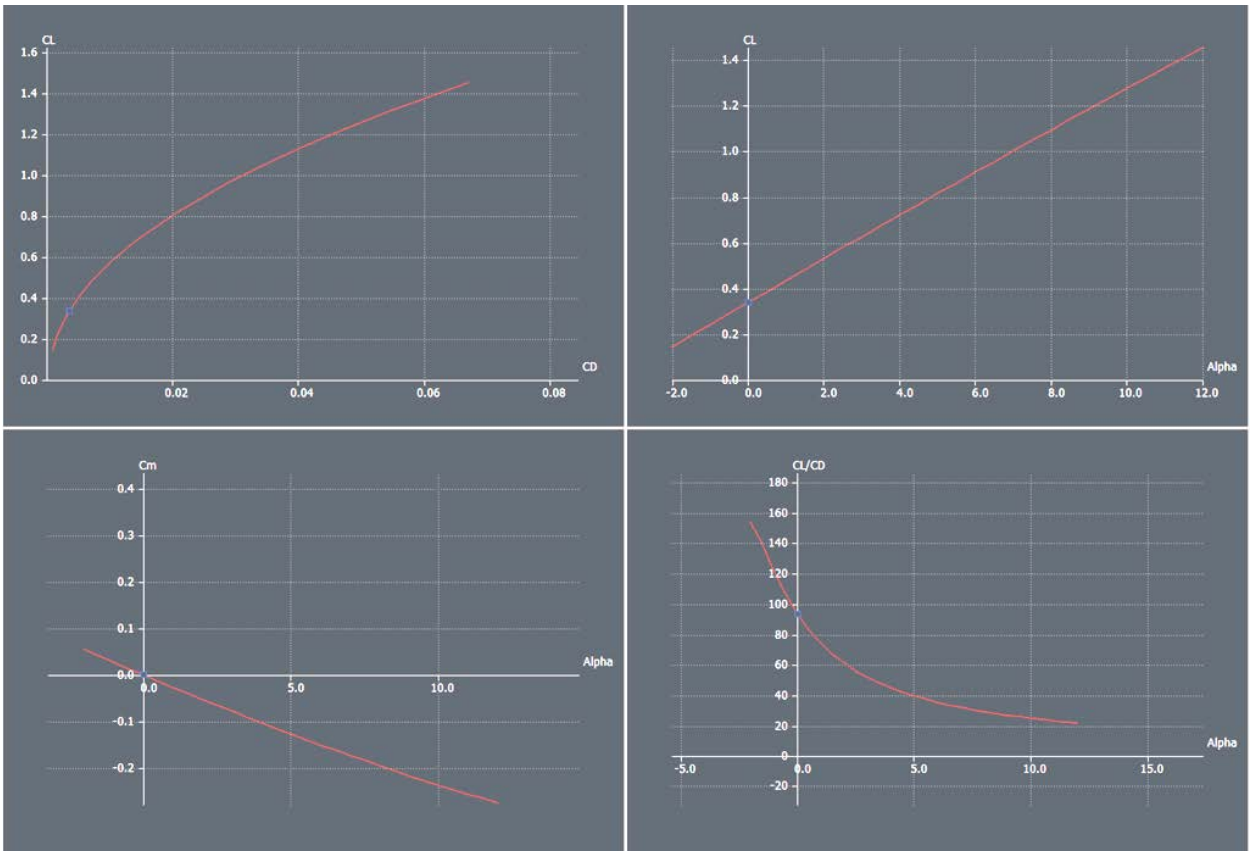

Graph 4.1: (From Top Left Clockwise) Drag Polar, Coefficient of Lift Distribution, Aerodynamic Efficiency, Coefficient of pitching moment distribution.

4.4 Landing Gear

The landing was constructed based on a previous plane's landing gear. We decided to go with a triangular formation of the wheels. The front wheel is angled at a 15 degree angle and the two rear wheels are angled at 30 degree angles. This formation was proven to be stable based on the levelness of the plane. The landing will be made out of aluminum or carbon fiber based on which is more resistant to the stress of the plane landing and being in contact with the ground.

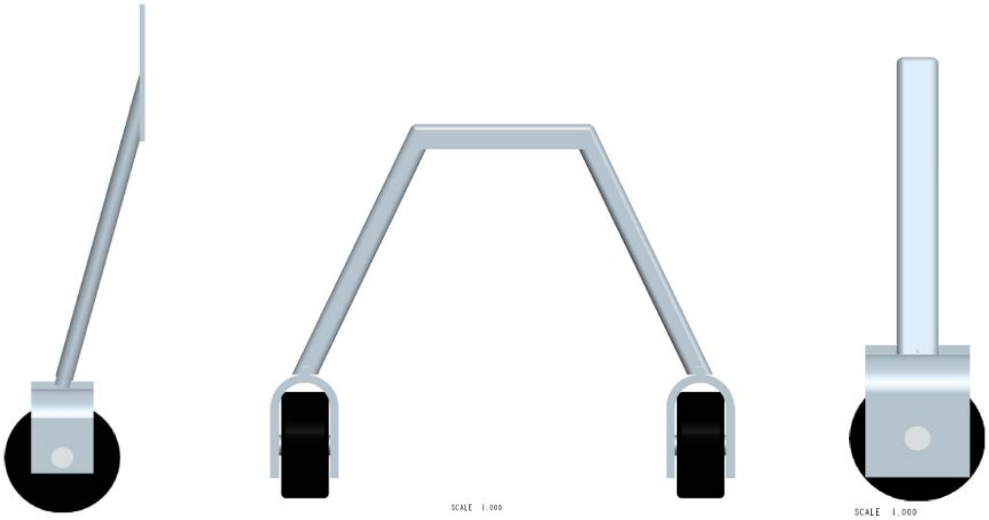

Figure 4.8: Landing Gear Design

4.5 Final Layout

After numerous iterations and configuration changes in the XFLR5 program, we came to a point where the conceptual design started showing stabilizing effects and we used this configuration as the final design. Although we have a final design, there are still numerous iterations that must be done to learn how stable our aircraft is during all phases of flight. This will be done during the break and into the next semester.

Wing	
Span	98 in
Area	6.7 ft-2
Root Chord	13.4 in
Tip Chord	6.3 in
Aspect Ratio	10
Taper Ratio	0.47
Sweep	0.27o
MAC	10.3 in
MAC Location Span-wise	2.5o
Wing Loading	2.7 lb/ft2
Cruise CL	0.34
Airfoil	NACA 4412
Ailerons	
Span	55-95% Half Span
Chord Percentage	20%
Max Deflection	±30o

Horizontal Tail	
Span	28.3 in
Area	0.93 ft2
Root Chord	6.3 in
Tip Chord	3.15 in
Aspect Ratio	6
Sweep	9.4o
Taper Ratio	0.5
Airfoil	NACA 0012
Elevator	
Span	Full Span
Chord Percentage	0.2
Max Deflection	±30o

Vertical Tail	
Span	20.7 in
Area	0.37 ft2
Root Chord	6.9 in
Tip Chord	3.45 in
Aspect Ratio	4
Sweep	14.04o
Taper Ratio	0.5
Airfoil	NACA 0012
Rudder	
Span	Full Span
Chord Percentage	20%
Max Deflection	±30o

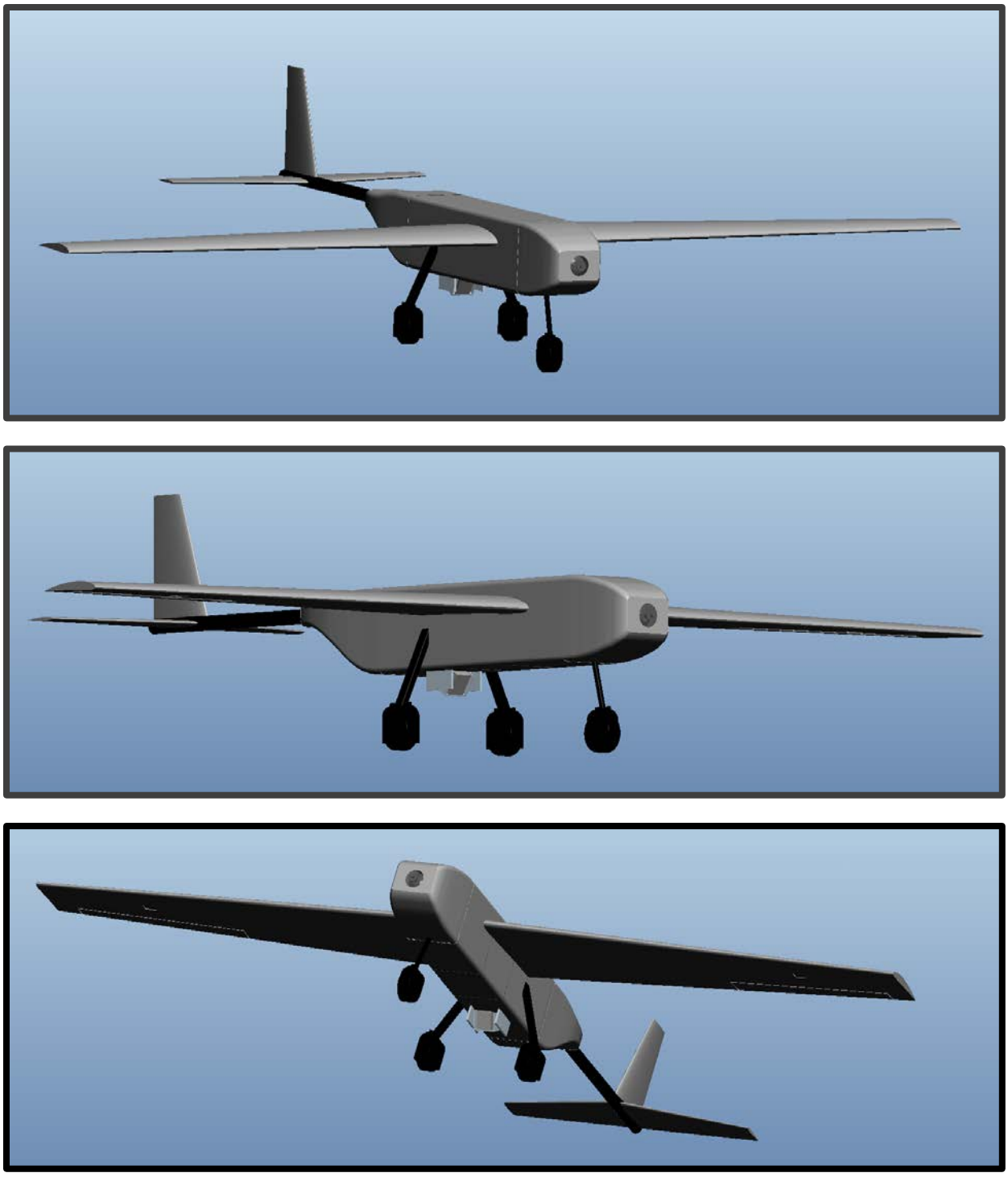

Figure 4.9: Final Configuration Layout

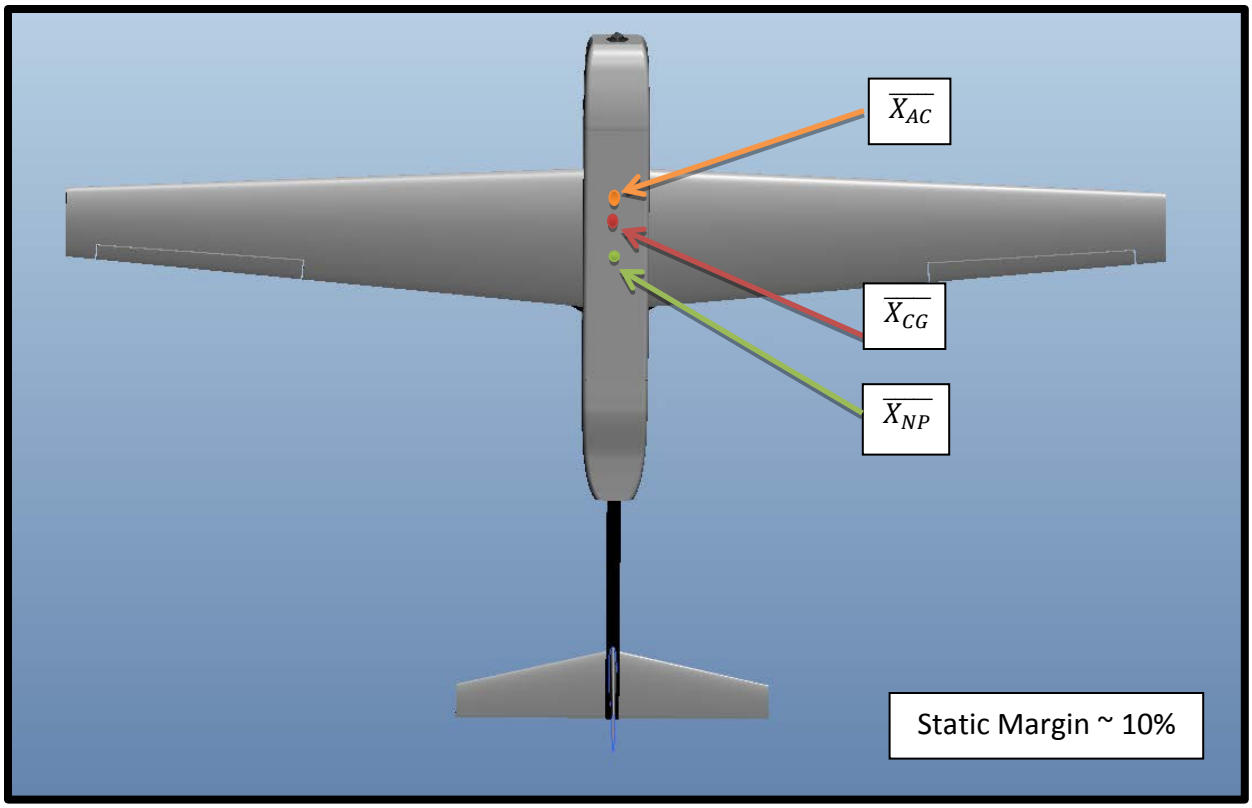

Figure 4.10: Determination of Static Margin

5.0 Aircraft Structure

5.1 Material Selection

Based upon the hybrid composite structure concept chosen earlier in the concept generation phase of the design, multiple fiber reinforced plastic (FRP) matrix systems and core materials were selected for different components of the design. FRPs will be the main materials of choice throughout the aircraft because of their high strength to density ratios and ability to be molded into almost any shape. Where needed core materials of a lower strength and density will be sandwiched between layers of FRPs to provide greater structural stability without a large increase in weight. One location that will not utilize composite construction is the center plate inside of the fuselage which will be constructed of plywood. Plywood is being used so that payload components can be easily attached to the internal structure and there will be no interference with the electronics in the payload. More specifics of material use will be discussed later.

Two types of fiber reinforcement, carbon fiber and fiberglass, were chosen while a single type of epoxy resin system was chosen to create the plastic matrix. Different fiber reinforcements were chosen so that specific properties could be tailored for each segment of the aircraft. The West System 105 epoxy resin was chosen for its high cure strength, moisture resistance, structural and chemical stability, and ability to bond well with both wood and composite fabrics. The epoxy resin system comes in two parts as the resin itself and a hardening agent. These two parts need to be mixed exactly to ensure a proper cure, which can usually be a problem but is made easy with pumps supplied in the West Resin System that measure out exact ratios of the two chemicals.

The carbon fiber of choice was a 3k 2x2 twill weave, meaning that three thousand filaments make up each fiber and every fiber runs over two then under two other fibers in the weave. Carbon fiber has a higher strength and stiffness while also possessing a lower density than fiberglass. It is however not as flexible as and greater in thickness than fiberglass, meaning that it is harder to form on curved surfaces and has a higher tendency to develop inclusions of air in the matrix. These factors, and the fact that it is four times more expensive than fiberglass per yard, limit the use of carbon fiber to structural members that require the higher strength and stiffness properties.

The fiberglass of choice is 120 E-glass, or 4hs satin weave fiberglass. This fiberglass is of an extremely tight weave with low thickness and high flexibility.

The core materials used for the sandwich structures and wings will be standard aircraft balsa wood, utilized in almost all RC aircraft applications, and expanded polystyrene foam. The balsawood will be used inside of the fuselage ribs because of its ease in shaping through the

use of laser cutters, and foam will make up the core of the wing. Using these core materials in conjunction with the FRP outer skins will drastically reduce the weight of the plane without compromising structural strength.

Material	T. Strength 0o/90o (KSI)	T. Modulus 0o/90o (MSI)	In-Plane Shear (KSI)	Poisson's Ratio
Carbon Fiber	87	10.1	13	0.11
Fiberglass	23	2.18	3.95	0.1

Table 5.1: Typical properties of fiber reinforced epoxy matrices

5.2 Fuselage

The outer skin of the fuselage will consist of four layers of fiberglass impregnated with epoxy resin, layed down with the second layer at +45^{o}, the third at +90^{o}, and the fourth at -45^{o} where all angles are relative to the first layer of fabric. This skin will be bonded to an internal support structure, pictured below, with quick hardening epoxy. The support structure was modeled after traditional RC aircraft internals and other aircraft created previously in the AUVSI SUAS competition while keeping in mind the increased structural stiffness from the multi-layer outer skin.

The center plate of this structure will be constructed of 3/8" plywood as discussed earlier while each rib will be constructed of balsa wood and a layer of carbon fiber in the sandwich core style. The rib at the front of the structure, where the nose cone connects to the fuselage, is termed the firewall. The firewall is a solid piece that acts as both a mounting point for the motor and nose cone, and a shield from heat and electrical interference generated by the motor. The two center ribs act as support for the wing structure and connection points.

5.3 Wings

The wings will consist of a fiberglass outer skin of four layers, layed up in the same style as the fuselage, with an EPS foam core. There will be two spars running through the wing from the tip chord to 6" before the root chord where they will be fitted to the shear box with epoxy. The spars act as the main support for the load felt by the wetted area of the wing, where the load is transferred from the fiberglass skin to the foam core and then into the spars, but the

fiberglass skin will absorb some of the tension forces and the foam core will do the same with compressive forces.

With the requirements of high mobility and ease of assembly in our design it was decided that an easy way of attaching and removing the wings for storage was necessary. This system all needed to be strong enough to safely handle the highest loads felt by the wings. Our solution to this was to have two solid rectangular bars of carbon fiber running through the fuselage and into each wing. These connectors will be rigidly attached to the frame by epoxying them to the two central ribs. Inside of the wing is a shear box made of carbon fiber that matches the profile of each connector and the aligning wing spar. The connectors will be press fitted 6” into these shear boxes until they meet the spar that has been fitted into the other end of the box. The front connector has dimensions of 0.654”H x 3/8”W while the rear connector has dimensions of 1/8”H x 0.40”W. Identified in the picture below are the two wing connectors.

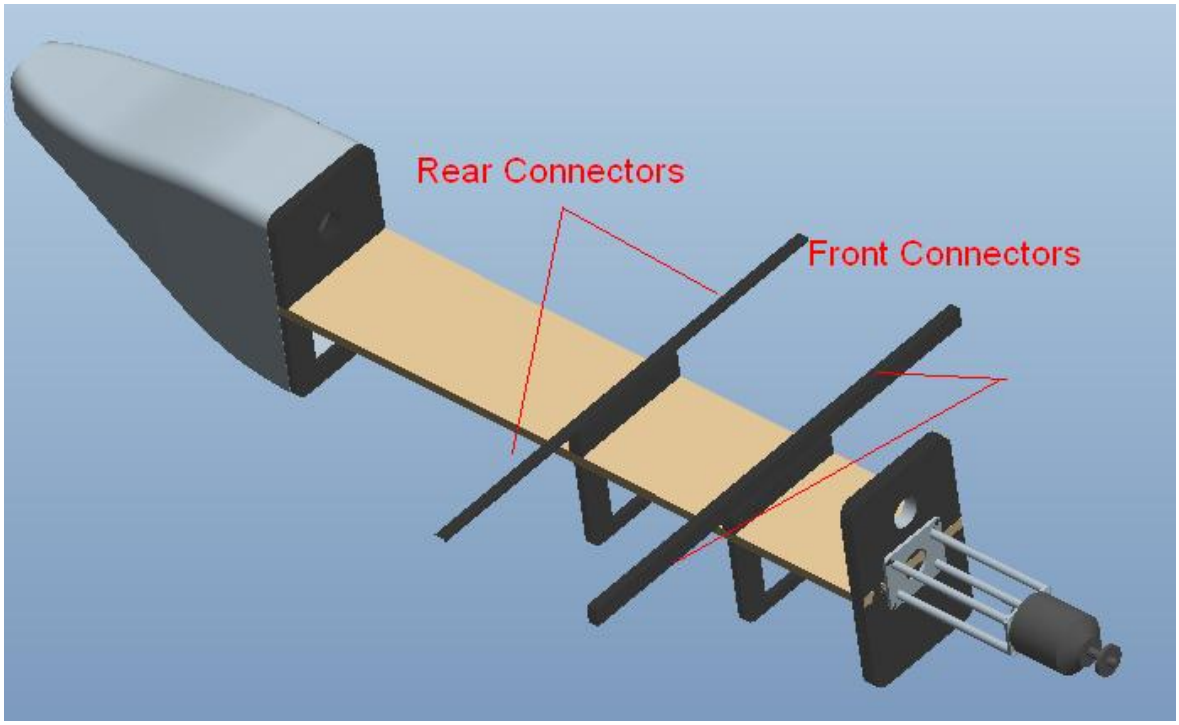

Figure 5.1: Front and rear wing connection points

5.4 Shear Box

The shear box is constructed of four layers of carbon fiber, mimicking the alternating layers of the wings and fuselage in a 0^{o}, $+45^{o}$, $+90^{o}$, -45^{o} pattern, with the front and rear being sized to fit the wing connectors. The front shear box has outer dimensions of 0.75”H x .471”W and the rear shear box has outer dimensions of .2”H x .471”W. There will be a section cut out of each wing core that will fit the outer dimensions of the box so that it can be secured into place by epoxy.

5.5 Wing Spars

The spars are made of multiple layers of carbon fiber to better support the combined compressive, tensile, and shear forces that they encounter. They are placed at 25% and 70% of the chord length from the leading edge to fit with the taper of the wings and the area removed from the wings by the aileron. The spars are rigidly attached 1” into the shear box with epoxy. After the shear box the front spar takes on the outer dimensions of the shear box for another 8” and then tapers to 50% of the outer dimensions at the wing tip chord. The rear spar begins to taper immediately after the shear box to 50% of its dimensions at the wing tip chord. The front spar, which takes the majority of the load, runs orthogonal to the root chord surface while the rear spar follows the angle of the wing from the end of the shear box to the tip chord. The spars will fit inside of cavities cut into the wings by the foam core manufacturers and will be joined to the foam with epoxy.

5.6 Tail Boom

The tail boom will be a unidirectional pultruded carbon fiber tube with an outer diameter of 1”. The boom will run from inside of the fuselage, attached to the frame at the rear rib, and have the tail section attached to the opposite end.

6.0 Structural Analysis

Because the spar structure and the wing connectors with shear box are carrying the weight of the plane, and lift forces generated by the wings, they are the most important structural members of the plane. A stress analysis was performed on each part to make sure that they will not fail under operating conditions.

6.1 Spars

The spar structures were created inside of Pro-E and then evaluated using the Mechanica Finite Element Analysis (FEA) module in a static stress analysis. This allowed for many reiterations in spar dimensions and shapes to be analyzed without refining and changing mathematical models for each. Standard meshing features were used with an 8% maximum error percentage added to the model. The positive load used in the simulations was derived from the maximum weight of the plane with payload subject to a worst case scenario acceleration of 4gs, while the negative load used was the max weight of the plane under 2gs of acceleration. These correspond to values of 76lbf and 38lbf respectively, while the load applied to the spar was cut in half assuming equal distribution between wings. This value, although outside the usual operating range of the aircraft and most likely never to be seen in its mission profile, was used to create a high factor of safety under all operating conditions. This was placed as a distributed load across the spar while the area connecting to the fuselage support structure had a rigid connection. Depicted below are the graphical solutions of the analysis.

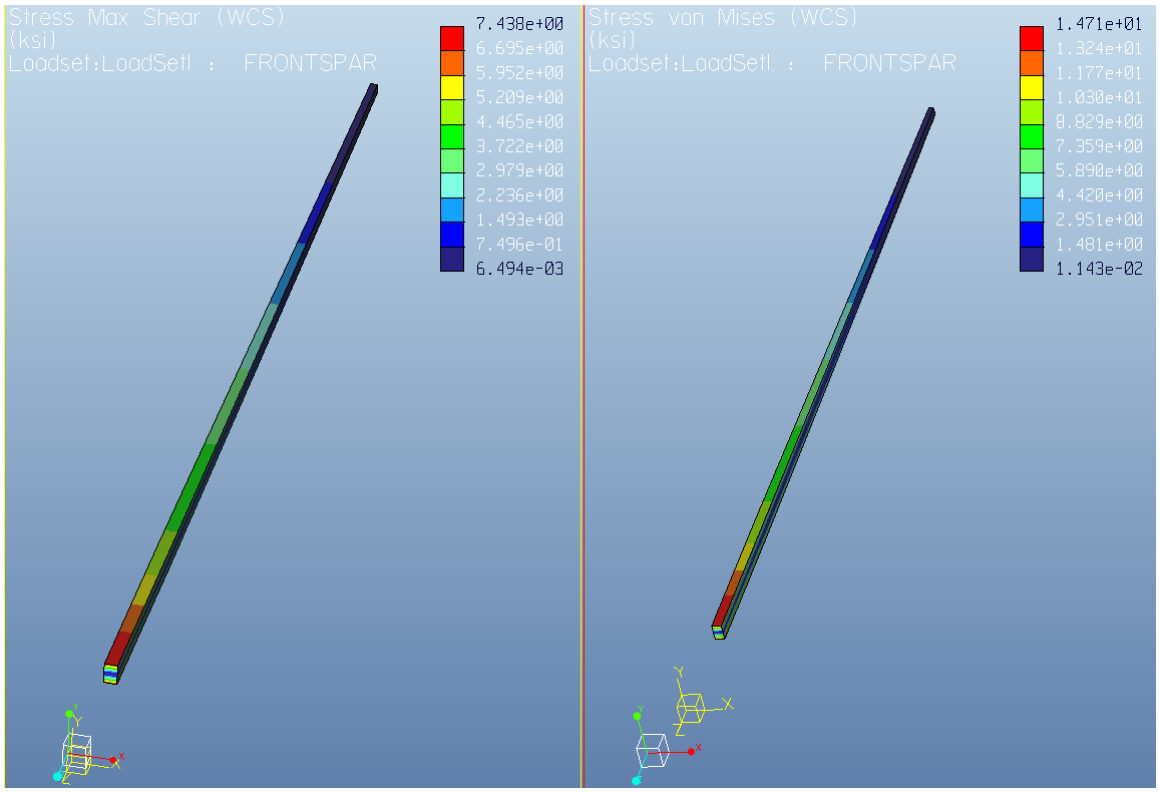

Figure 6.1: Mechanical Stress analysis of spar using a top load of 38lbf

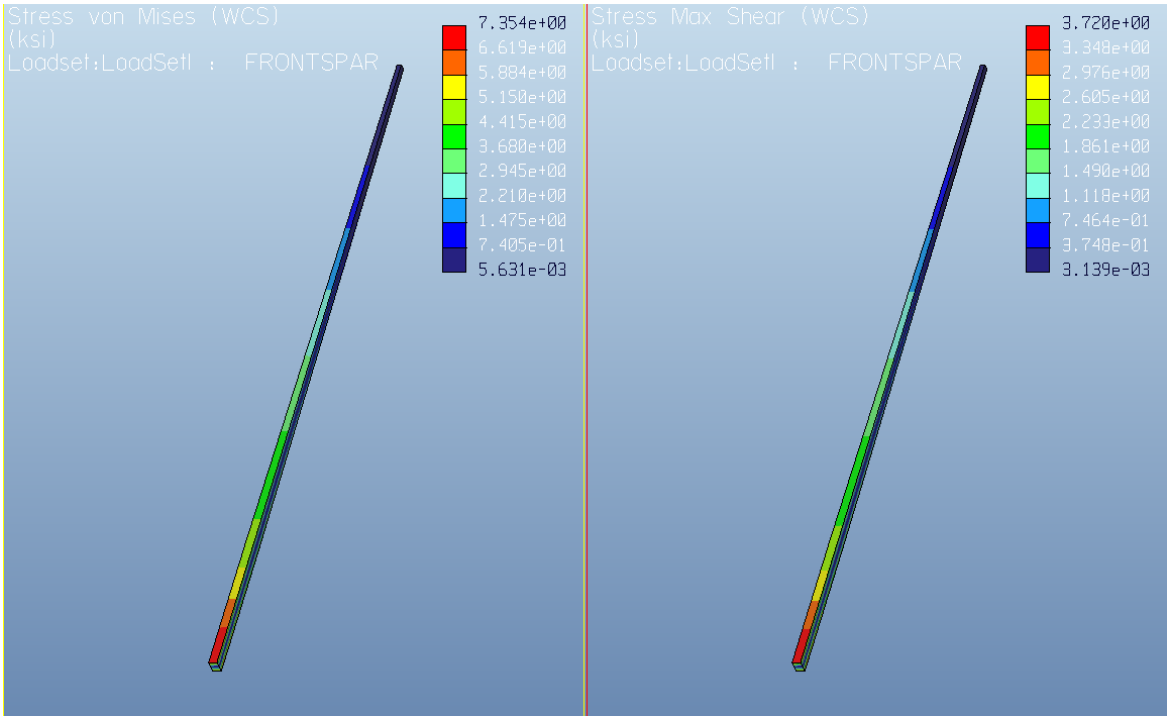

Figure 6.2: Mechanical Stress analysis of spar using a bottom load of 19lbf

As can be seen from the first stress analysis the highest shear stress reached in the spar is 7.44ksi and the maximum von mises stress is 14.7ksi. This provides a factor of safety of 1.75 for shear stress and 5.92 for the yield stress. The maximum deflection at the end of the beam under 38lbf was 1.98”. All of these values offer a very safe window of operation and are overestimations of what the spars will actually experience, as the foam core and fiberglass skin will absorb some of the stresses created.

6.2 Wing Connection

The wing connectors were evaluated in much the same manner as the spars. The bottoms of the connectors were treated as a rigid joint in their center section as they will be attached to the fuselage structure with epoxy. Below are graphical depictions of the stress analysis.

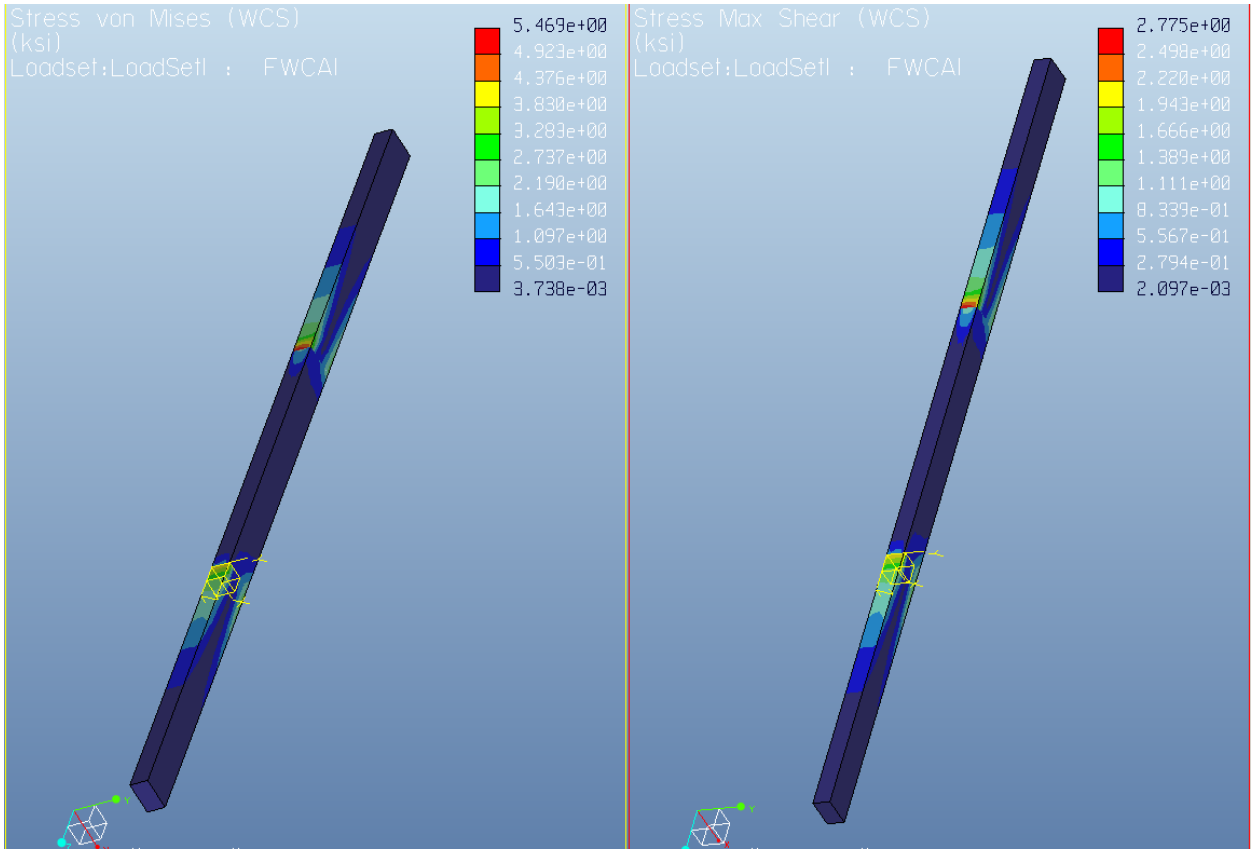

Figure 6.3: Mechanical stress analysis of the wing connector with a76lbf load

There are high stress concentrations at the points where the connector meets the edge of the fuselage but they are still well under the limits of the material. With a von Mises stress of 5.47ksi and maximum shear stress of 2.78ksi there is a factor of safety of 15.9 for yield and 4.77 for shear which is more than acceptable.

7.0 Fabrication Methods

Fabrication of the individual components will be slightly difficult without prior experience in composite construction, but all parts will be similar in construction and advising staff at the High Performance Materials Institute (HPMI) will be on hand. All wood components, including the core panels of the rib, will be cut into shape using a laser cutter in the STRIDE laboratory at the FAMU/FSU College of Engineering. This will provide exact dimensions with little inaccuracy in an easy to use manner. The foam cores of the wings will be custom cut by FlyingFoam to avoid the process of hotwire cutting the foam blocks into the proper airfoil shape and having to create the cavities for the spars and shear boxes.

7.1 Fuselage Fabrication

The fuselage will be constructed by first creating a plug of the fuselage. This is a solid body of either foam, wood, or another easily moldable material that can be cut or formed into the shape of the fuselage. The fuselage can be created around the plug if it is made of foam, because of the fact that the foam can be melted by an acetone solvent, but a mold must be created for any other plug material. This process is fast but provides less stability on flat surfaces and another plug will need to be created if there are problems with the end product. Because of this we will be creating molds of the fuselage.

To create a mold of the plug it must first be coated with a peel ply fabric. After this the entire plug will be sprayed by a coating of a polyvinyl alcohol (PVA) release film so that layers placed over this can be easily removed. Once the film sets layers of composite fabric will be layed over the plug. Each layer must be covered and saturated with an equal amount of resin, which must be first mixed in the proper ratios with its hardening agent, and then run over by a roller to make sure the layer is properly fitted and no air pockets remain. This will be repeated till a thickness at least 8 to 10 times that of the part is layed over the mold. Another coating of the PVA release film must now be sprayed on the mold and a layer of peel ply placed over once the release film has set. The mold is now ready to be vacuum bagged. One side of the mold should be wrapped in the vacuum bag material, which should extend slightly past the mold, while the vacuum pump tubes are placed at the ends of the mold in the extended bag area. The other side of the mold should now be wrapped in the vacuum bag material and pressed tightly onto the surface. All possible air pockets should be removed and the outer edges of the bag

sealed with the proper tape. As an extra measure portions of the vacuum bag should be clamped with vices. When the pumps are run and all air is evacuated from inside of the bag the mold is ready to set. A cure time of at least 24 hours is recommended for the West Systems resin chosen.

Once the mold has cured it can be easily removed from the vacuum bag because of the peel ply layer. The mold should be cut from the plug and cut in half so that a female mold of each side of the plug is now open. All excess fiber should be cut or sanded from the mold and the face of the mold should be checked for imperfections.

If the mold is now fully prepared and clean the fuselage construction can begin. The process for creating the fuselage is identical to that of the mold around the plug, except that the fiber layers are now wetted to the inside of the mold instead of the outside. The same vacuum bagging process applies as before.

7.2 Wing and Tail Section Fabrication

The wings will be formed much the same as the mold around the plug where the foam core is taking the place of the plug. In this case no PVA release film or peel ply layer is needed before laying the fabric. Before the fabric is applied the shear box and spars should be put into placed and joined to the core. The first layer will be wrapped around the wing in as few segments as necessary and a very slight overwrap where the ends of the fabric meet. This point should be at the trailing edge of the wing to reduce any separation effects that might occur. Once the fabric layer is layed it should be wetted with the proper amount of resin. Each following layer should follow the same procedure with overlaps changing sides. Once all layers have been placed a layer of PVA release film should be sprayed over the wing and once it is set the peel ply should be applied. The vacuum bagging process and cure time are identical to that of the fuselage.

7.3 Fuselage Rib Construction

The ribs of the fuselage will be formed in an identical manner to that of the wing. The balsa core should first be prepared by forming each 1/8” sheet of wood together in 90^{o} alternating patterns using epoxy. This will provide greater structural support in all directions for combined loading. Once the core epoxy is set the carbon fiber tape can be wrapped around the core. The tape should be saturated with resin and all surfaces of the rib pressed to remove air bubbles. A vacuum bagging process identical to that of the wings and fuselage can now be used. To save on material and time it is possible that multiple rib sections be placed inside of one vacuum bag.

8.0 Imagery System Design

8.1 Image System

The aircrafts payload will accompany an imagery system effectively providing a bird's eye view of the flight mission. Providing an onboard wireless video or image system provides many multirole capabilities to an aircraft such as intelligence, surveillance, reconnaissance, and rescue.

The imagery system design must be specifically tailored for this aircraft and mission profile. The proposed design must be able to identify several targets while flying along a Predefined search based on GPS waypoints. While flying at an altitude of 500 ft. the aircraft must be able to see targets directly on or up to 250 ft. off the GPS waypoint path. The aircraft will need to transition during the flight into an Area Search mode where targets may appear at any location within this area.

This image system should provide its operators a visual confirmation on targets either in real-time or upon recovering data from the aircraft. Under these requirements an imagery system must be chosen and modified in order to meet the criteria above. The images taken or received must accurately capture the target characteristics. The camera system should also be lightweight by design and easily mounted to the airframe. This system must include a varying field of view in order to capture targets beyond visible sight. Images taken from the air will need to either be transmitted directly to the ground station or be stored safety till the aircraft lands.

8.2 Problem Description

As specified in the competition description, the targets on the ground will be geometrically shaped and display alphanumerics. Each target will be a different colored shape with dissimilar alphanumerics. The minimum dimension of the target (length or width) will be 2 ft. with a maximum of 8 ft. The sizing of the alphanumerics will be sized to occupy 50-90 % of the length/width and between 2-6 inches in thickness, and will vary in color and contrast.

Figure 8.1 Alpha numeric Ground Targets

The camera design should primarily be able to distinguish the target characteristics from the specified flight altitude, while remaining lightweight as possible. The camera system must have at least ± 60 degrees horizontal and vertical FOV. The camera resolution will be limited if a downlink system is used. The camera will need a gimbal system to adjust the FOV during the flight as well as a control system on the ground to operate the gimbal. There is an abundance of commercially available camera systems, but few that meet the requirements of the mission profile. The two main possibilities to capture, send and process images are to either use still-image camera pictures or implement a real-time video display. Both choices have immediate advantages as well as disadvantages to the unmanned aerial system.

8.3 Problem Solution

One advantage of a standard camera is that it requires far less transmission data than a constant data feed. Pictures with a still camera are usually captured at a much higher resolution than a video camera. Also the camera will require far less transmission power to send less data. In contrast, a still-picture camera is required to take many pictures to capture the target. The user will need to implement multiple cameras or apply a gimbal system to change the cameras viewing angle. Still images will not be updated as quickly as a live video feed and could possible cause a delay in changing the camera position. In this case, the target could easily be missed. Target acquisition will most likely take longer than normal opposed to a constant data feed. Many still image camera systems provide a higher resolution than CCD video cameras.

Implementing a live video stream allows the user to constantly update their position for an immediate target acquisition. This technique shortens the amount of time required to find a target as well as makes shorting images much easier. These video systems are similar to security cameras or machine vision cameras. They provide a lightweight design that is easily mounted to a gimbal. Unfortunately, constant data feeds require much more power than a still image system, and must be transmitted at a higher frequency, most likely in the gigahertz range to maintain a 6-8 Mbit/sec bit rate. Video stream technology also requires a clean signal for

operation as well as real time image stabilization, which can be implemented by adding padding around the camera/motor or using gyro-synchronization.

8.4 Camera Selection

In this section many different types of commercially available off the shelf cameras were compared and graded based on the following parameters. The cameras were graded on a scale from (1) poor to (5) outstanding in each category.

Camera Selection Parameters Criteria	weight
Weight	20%
Mounting	8%
Resolution	15%
Zoom	10%
TX Ability	8%
Price	15%
Toughness	5%
Power Req.	10%
Dimensions	9%
Total	**100%**

Table 8.1: Camera Selection Parameters

Camera Decision Matrix Criteria	weight	Nikon D300 DSLR Grade	Nikon D300 DSLR Weighted G	Sony KX-181 HQ Grade	Sony KX-181 HQ Weighted G	Sony FCB Block Grade	Sony FCB Block Weighted G	Axis 212 PTZ Grade	Axis 212 PTZ Weighted G
Weight	0.2	2	0.4	5	1	4	0.8	3	0.6
Mounting	0.08	3	0.24	3	0.24	4	0.32	5	0.4
Resolution	0.15	5	0.75	3	0.45	3	0.45	3	0.45
Zoom	0.1	5	0.5	0	0	5	0.5	3	0.3
TX Ability	0.08	3	0.24	3	0.24	5	0.4	4	0.32
Price	0.15	1	0.15	5	0.75	3	0.45	2	0.3
Toughness	0.05	4	0.2	1	0.05	2	0.1	5	0.25
Power Req.	0.1	5	0.5	4	0.4	3	0.3	3	0.3
Dimensions	0.09	1	0.09	5	0.45	3	0.27	1	0.09
Total		**29**	**3.07**	**29**	**3.58**	**32**	**3.59**	**29**	**3.01**

Table 8.2: Camera Decision Matrix

After analyzing several different camera configurations it was determined that a live video feed would be a better alternative than retrieving images from an SD card. Cameras such as the Nikon DSLR would be unacceptable for this mission because its heavy design and inability to send images without the addition of a wireless USB module. The Sony KX-181 camera is a very inexpensive analog camera that is lightweight and is commonly used on RC aircrafts.

It was determined that the Sony FCB Block Camera was the best choice for the mission requirements. The IX11A Block Camera has the capability of sending the images as analog Video Blanking Syncs (VBS) and a high-speed serial interface with TTL signal-level control (VISCA protocol). This camera has 18x optical zoom capability and an analog resolution of 520 TV lines. The FCB Block Camera also gives the user the ability to customize an On-Screen Display (OSD) which would be used for information such as heading, airspeed, altitude, and GPS coordinates. If permitted by budget constraints, a second test camera would be purchased to test communications equipment as well as be available for use if the main camera failed.

8.5 Downlink Selection

Sending images or video streams wirelessly to the ground station is a very challenging prospect, but equally advantageous in order to determine target characteristics in real time. The communications equipment must provide enough bandwidth to support the camera downlink. The bandwidth requirements become a very challenging problem when capturing high resolution images. Using this method the video signal would be converted to analog signal which contains luminance, brightness, and chrominance. These combined channels create a composite video connection known as NTSC standard. Analog video signals require less bandwidth that that of a digital signal, but are also more susceptible to transmission noise. This can particularly be problematic if implementing autonomous detection software. These static losses in the video feed would create several false positives.

Use of a digital downlink for transmitting a live video feed has many potential advantages; if using an image recognition system the feed would not need to be converted before processing, and the downlink connection would receive less interference. While analog signals require amplifiers digital signals do not. These amplifiers add distortion and noise which damages the signal.

One of the most important features about implementing a video transmission system is its ability to see targets in real time. Based on the chosen camera, Sony FCB IX11A, and its maximum resolution it is possible to determine the average file size produced. Since targets will be colored grayscale images are not possible. Therefore, images will be based on the 24-bit color scheme in which each pixel contains 9 bits. Multiplying the maximum resolution by the number of bits each pixel contains gives the average file size of 3.3 Mb. Directly sending this data to the ground station is possible using a very high speed modem.

As a benchmark the SRM6100 Wireless Serial Modem was used from Data-Linc Technologies, this modem has an average RF transmission rate of 166 Kbit/s. By dividing the

image size by baud rate one can determine the transmission time. In this case a 3.3 Mb file would require 2 minutes and a half minutes to be transferred.

$$(Effective\ Resolution) * (24 - bit\ color\ image) = Max\ File\ Size$$

$$\frac{File\ Size\ (Mb)}{Baud\ Rate\ (bps)} = Transfer\ time\ (s)$$

During the Enroute search the aircraft will be travelling at approximately 45 miles per hour, which means it will be covering 66 feet per second. Using these transmission parameters the ground station would receive an image every 1.875 miles. Clearly, the transmission of data to the ground station is too slow to accurately find and locate targets. This means that that the images would need to be compressed before being sent, which requires an on-board microprocessor to compress the images before being transmitted. Although there are many advantages to using a digital transmissions it was decided that analog video transmission would be a better option.

8.6 Antenna Selection

Antennas can be described as a metallic device conducive for radiating or receiving radio waves. RF communications are modeled the isotropic radiator principle, where the radiated pattern is a perfect sphere in all directions. Antennas are measured by their gain in which an isotropic radiator would have a gain of 0 dB. Gain is directly correlated to the directivity in which an antenna radiates. This means higher gain antennas have longer range, but a narrow reception window; effectively narrowing the signal to improve distance. For this particular aircraft and mission profile the coverage area could be a radius of up to 3 miles. The exact flight path remains unknown until several hours before the mission. Under this criteria the antenna must not high gain. In this particular situation there is a level of ambiguity of where the aircraft will need to fly. Implementing a high gain antenna could easily lose the signal if the antenna was not pointed directly at the aircraft.

Antennas come in different configurations and polarizations. Polarization is the orientation of the electric field in respect to the earth's plane. Polarization is based on the physical structure of the antenna design which directly related to its ability to transceive signals.

The behavior of radio wave polarization is assumed to be elliptical. Such that the waves vary over time period. This elliptical pattern general converges two either a straight line (linear

polarization) or a circle (circular polarization). Different mounting orientations dictate the radiation pattern of the antenna. Generally, linear polarized antennas are mounted either horizontally or vertically. Vertical polarization is the most commonly used orientation because of its omni-directional radiation pattern. This form of polarization has an electric field perpendicular to the Earth's surface. Vertical polarization is used to broadcast radio waves such as WiFi and AM/FM radio. While horizontally mounted antennas have an electric field parallel to the Earth's surface and are used in television transmission modules.

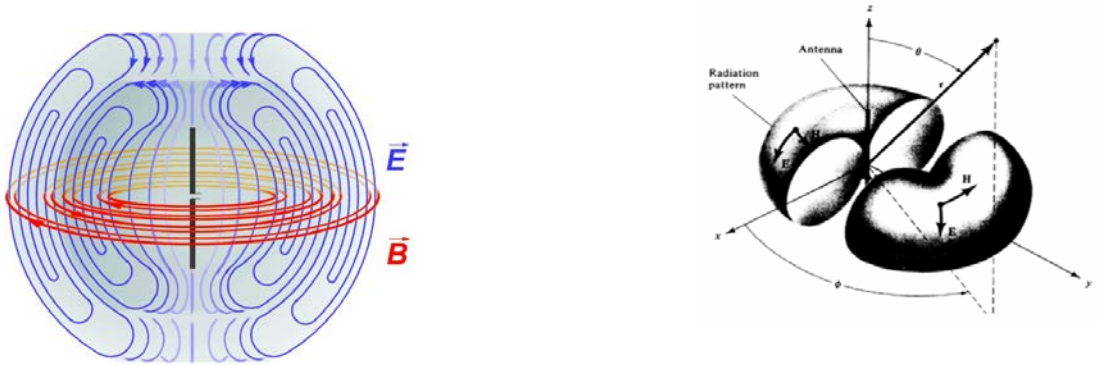

Figure 8.2: Dipole Antenna Radiation (Left) and Omni Directional Antenna Radiation (Right)

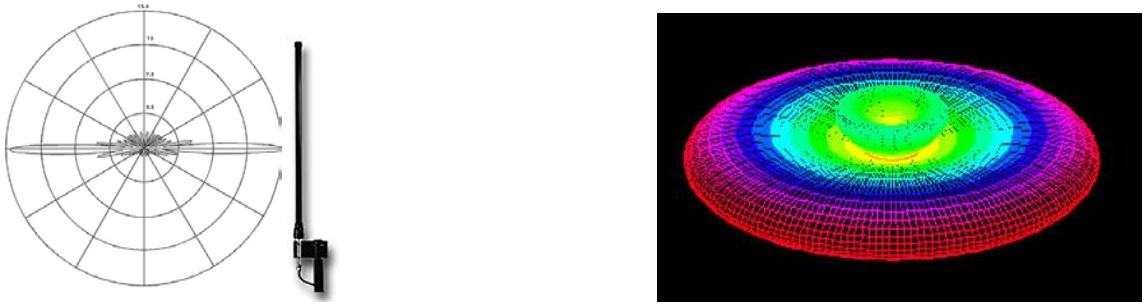

Figure 8.3: Vertically Polarized Omni-directional Antenna 2D and 3D

Figure 8.4: Horizontally Polarized Omni-directional Antenna 2D and 3D

There are several other antenna configurations available, but these two types were the most optimal choices for the aircraft and the ground station. At a operational point to point distance of 3 miles an omni-directional antenna on the aircraft would provide a large operating margin for the transmission signals. In order to receive the signals from the aircraft on the ground station a powerful antenna will be needed to recover the video feed. The grid antenna design is a solid mid-ground platform that balances distance and reception angle. The necessary gain on the grid antenna will be between 9 dB and 24 dB based upon the operational signal margin. At a maximum a 24 dB antenna can recover a signal from up to 6 miles.

Choosing the appropriate antenna system is entirely based on the propagation of radio waves and the following factors:

- Free space path loss: The geometric spreading of the signal wave causes a drop in signal power.
- Signal power degrades as the wave propagates through solid objects such as trees, walls, glass, etc.

According to the Radio Communications Class License 2000, Item 26 transmitters operating between 2400-2450 MHz must not exceed a maximum Effective Isotropic Radiated Power (EIRP) of 1 watt in the use of telemetry purposes. The purposed 2.4 GHz video transmission system hereby abides by these guidelines having an operational power output of 500 mW.

8.7 Image Geotagging

As part of the flight mission requirements the targets GPS location must be identified. This process can be done in a number of ways using technologies such as a laser range finder. Due to the strict weight requirements of the aircraft the GPS coordinates (longitude and latitude) will be calculated with a simple trigonometric equation. Assuming the target appears at the same elevation that the plane, and given the pan/tilt camera angles the x and y distances can be calculated. The equation below describes how this is computed using a simple diagram.

Figure 8.5: A Common Range Finder

The goal is to calculate the Euclidean distance, and determining the GPS coordinates in reference to the aircrafts heading. The altitude is read from the GPS sensor sent to the Paparazzi board. The camera servos are controlled by the autopilot board as well. A custom GUI on the Paparazzi ground station will need to be designed that allows manual control of the camera servos by using PWM signals. These signals will be counted and calibrated such that the pan / tilt angles correspond with the PWM signals sent to the motors.

$$\tan(\alpha) = \frac{x}{h} \quad \tan(ß) = \frac{y}{h}$$

$$x^2 + y^2 = ground\ distance^2$$

Using this information the GPS coordinates of the target can be determined. Although, thorough testing is necessary to see how accurate the results are; a proposed test is flying the aircraft over a known location and using linear regression in determining the associated error % in the calculation.

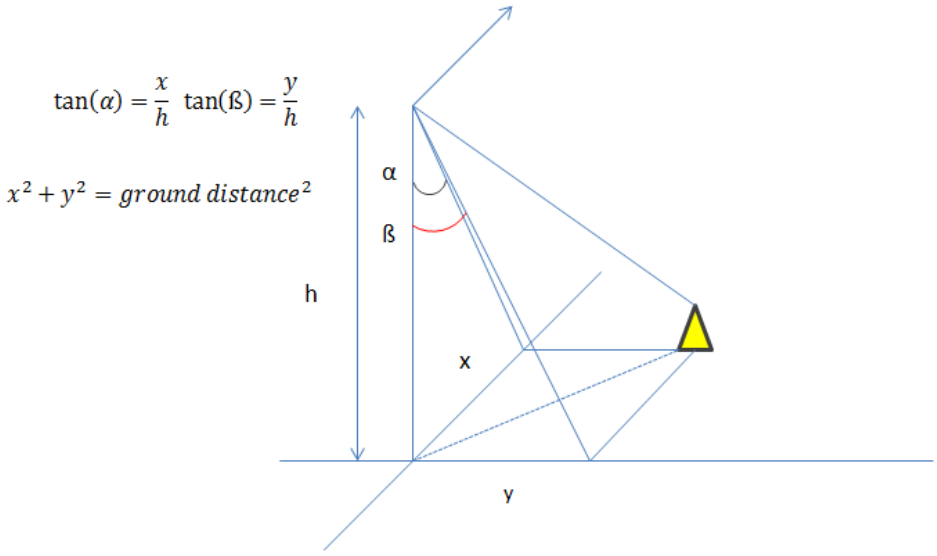

Figure 8.6: Euclidean Distance Diagram

8.8 Complete Design Detail

In order to communicate with the ground station there will need to be three communication links established between the ground station and the UAV. Each of these links serves a vital purpose of brining data from the aircrafts sensors or imagery systems to the ground station.

The process of sending images wirelessly to the ground station is one of the most critical features of this aircraft platform. The downlink must provide a clear and interference free link to the ground station in a rather short period of time. The video feed from the UAV will be sent as analog signal, which have a much requires a much smaller baud rate. The transmitter and receiver hardware were chosen based on the broadcast range, baud rate, frequency, and cost. A 2.4 GHz wireless video receiver was chosen to match the transmission frequency. Although due to range requirements the addition of a high powered antenna will be necessary. Augmenting the video receiver with a high powered antenna will require a signal amplifier before entering the receiver. The amplifier will allow a weak radio signal to be detected by amplifying the antenna signal. Figure # shows chosen imagery downlink system configuration.

It is very important to understand the possible roots of problems when building wireless communication systems. Having multiple transmissions sent at different frequencies at variable locations based on ever changing weather patterns can be very unpredictable. The wireless communications must be tested on the ground several times before going airborne and will change based on the physical features of the aircraft as well.

The Imagery system will be mounted on the underbelly of the aircraft between the landing gear. The Sony FCB IX11A Block Camera will be used for specific purpose of target recognition during flight. The camera will need a gimbal mount with dual servos to pan and tilt in two directions. By changing the FOV the camera can effectively see 180 degrees horizontally and over 60 degrees vertically.

Since frequent remote testing will be necessary the camera will be powered by a dedicated Lithium Polymer battery. The voltage requirements for the battery change depending on the zoom servos, but at maximum the FCB block camera requires 12 V. The video will be captured by the ¼ Exview HAD CCD sensor and be sent as an analog signal to the ground station. This camera is equipped with 40x optical zoom making it extremely capable of determining the targets from an altitude of 500 ft.

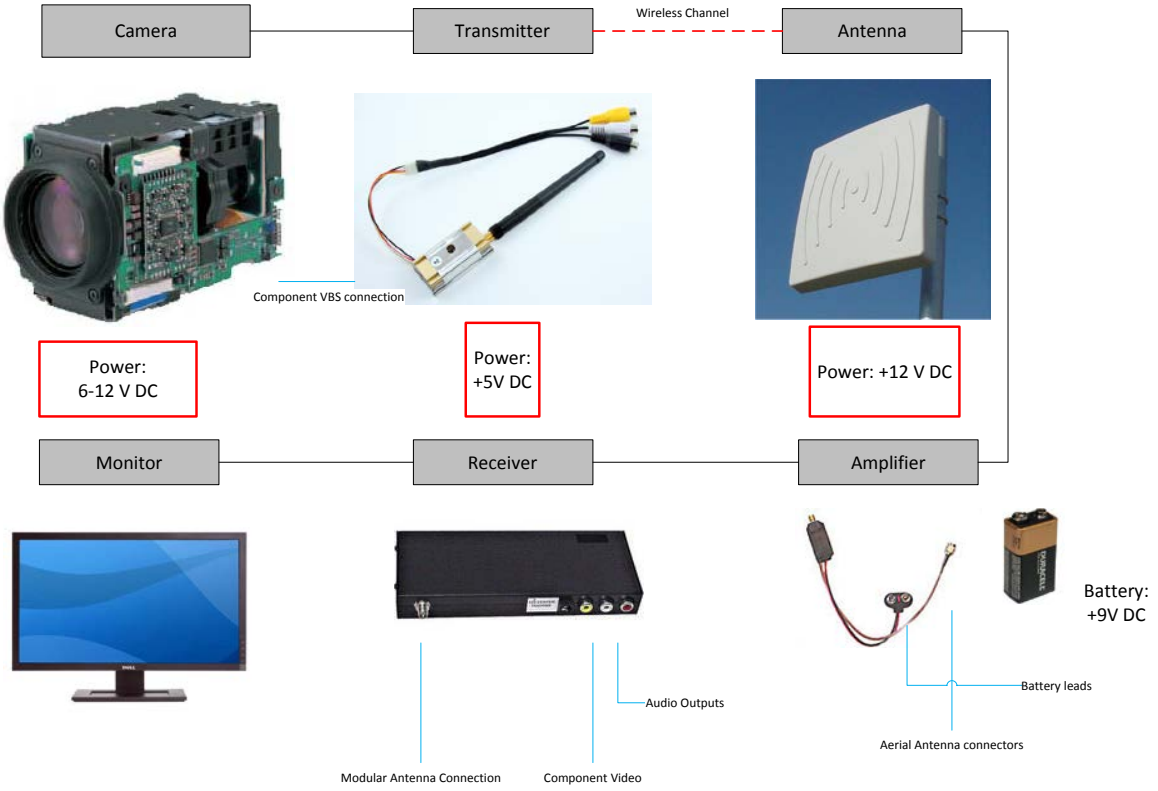

Figure 8.7: Imagery Downlink System Configuration

8.9 Frequent Communication Problems

It is very rare that wireless communication systems work perfectly. Changing locations and whether conditions can often reveal problems in the system. This section outlines many commonly experienced problems in wireless communications. Once the testing phase begins these parameters will need to be examined thoroughly.

Electronic components such as the autopilot, motor, or other wireless signals can generate signal noise that interferes with the video feed. Each of these interferences can easily cause the video signal to become completely unintelligible to the receiver. Even the slightest noise from the aircraft could limit the ground station from performing image processing by creating false data.

External sources are generally a contributing factor based upon the operating location of the aircraft and the broadcast frequency. Global System for Mobile Communications (GSM) operates between 900-1800 MHz. More specifically the wireless video feed could be damaged by WiFi, which operates on the 2.4 GHz band. Even the presence of high voltage power lines is a potential source for interference.

Narrow Band Interference is directly caused when attempting to broadcast multiple devices on the same frequency. Narrowband interference causes a drastic reduction in the signal to noise ratio. Operating multiple devices on the 2.4 GHz band would be catastrophic, as seen by many RC enthusiasts. Although, by design the Autopilot and RC module are being operated at 900 MHz. It is possible that this may cause problems, but the autopilot most likely would not be transmitting data from the sensors if the manual over-ride was enabled.

It is possible to dramatically lower the signal strength of the wireless communication links, in both the video and autopilot transmissions, by placing them near high power sources. Therefore, placing the transmitters near the motor could potentially power the signal reception. This is called Receiver Inundation. Specific high density and/or conductivity materials are able to shield electromagnetic waves. Some of these materials are carbon fiber, copper, and aluminum. It is critical to mount the transmitter antennas outside the fuselage and away from these particularly harmful materials. The loss of signal can be greatly influenced by creating multiple paths with the electromagnetic waves. This process, called Multipathing, commonly occurs when RC signals reflect off smooth and conductive surfaces creating multiple signal paths that effectively interferes with signal reception.

9.0 Avionics System Overview

As mentioned before, the SUAS needs to complete waypoint navigation and an area search autonomously. This task is accomplished using an autopilot system. The autopilot system will handle the autonomy using several sensors and a program that is loaded onto a microcontroller that interfaces with the sensors. The system is broken up into two main parts: the autopilot board and the sensors.

The autopilot board is the main and most important part of the autopilot system. All of the information from the sensors is sent into the autopilot board via direct connection. Using the data received, the autopilot program will make decisions in real time. The program is where the autonomy is handled as there is no user input while flying. The program will execute a preloaded flight plan using the sensors interfacing to it.

There are multiple sensors that need to interface to the autopilot board for the mission to be completed. The first and one of the important sensors is the GPS. The accuracy is important and should be no greater than 100ft due to the mission objectives. The GPS sensor also needs to refresh the location at a rate no slower than every one second. The next important sensor is one that measures the attitude (orientation) of the aerial vehicle. The two main methods to accomplish this are using infrared sensors or an IMU. The other sensor is the airspeed sensor.

The communication between the on board autopilot and the ground control station will need to be interfaced to the autopilot board. The two main parts to the communication are the data communication between the GCS and autopilot board and the other communication is the R/C receiver that the autopilot board takes commands from.

9.1 Autopilot Board

The autopilot board is the most important part of the autopilot system because it controls the plane based on the data it collects. The autopilot board is the board that all the sensors interface to and where the autopilot program is stored. The program will make decisions on whether to change altitude or heading based on the preloaded flight plan. Data will be relayed back down to the user. The user will be able to see it in the ground control system graphical user interface.

When selecting an autopilot board, there a few important factors to consider. The power usage, size, board layout, ground control system, and flight simulator need to be looked at for each board being considered as these are all important factors. The power usage and size are obvious factors because the aerial vehicle will be running on a limited amount of power, so

the less power used the better. Also, since the aerial vehicle should be as light as possible the autopilot board should be as small and light as possible. The board layout has to do with the way the input and output ports are set up. For example, an autopilot board with no servo controls would be a very poor choice because there would be no way to control the flaps on the aerial vehicle. The ground control system is the interface between the aerial vehicle and user. The flight simulator is used to see how the user's aerial vehicle will handle flying. This is a good way to test new designs.

After searching through various autopilots, there are two main autopilots that are going to be looked at: the Paparazzi Tiny v2.11 and the Ardupilot Mega. Both of these autopilots are made for small UAV's similar to the objectives of this project. They also meet our budget requirements because their board design is free to download along with their autopilot software. They both have websites with forums for support as well. Here is how both boards scored in a decision matrix designed around the five factors previously mentioned:

Autopilot Decision Matrix			Ardupilot Mega			Paparazzi Tiny	
Criteria	weight		Grade	Weighted G		Grade	Weighted G
Power Usage	0.2		3	0.6		3	0.6
Size and Weight	0.15		2	0.3		4	0.6
Board Layout	0.25		1	0.25		4	1
GCS	0.3		4	1.2		4	1.2
Flight Simulation	0.1		4	0.4		5	0.5
Total	**1**		**14**	**2.75**		**20**	**3.9**

Table 9.1: Autopilot Decision Matrix of Ardupilot Mega and Paparazzi Tiny v2.11

Based on table 9.1, it is clear to see that the Paparazzi Tiny v2.11 is the best selection to complete the mission objectives. The Tiny board is 70.8 x 40mm (about the size of a credit card) and weighs around 24 grams. The board has a variety of ports, including 8 PWM outputs, one USB, 8 analog input channels, and many others (Figure 3). The ground control station is will get the job done and is very customizable, allowing a user to add a variety of widgets to the display screen. The flight simulator is similar to many others, allowing a user to put in the specifications of their aerial vehicle and run the simulator.

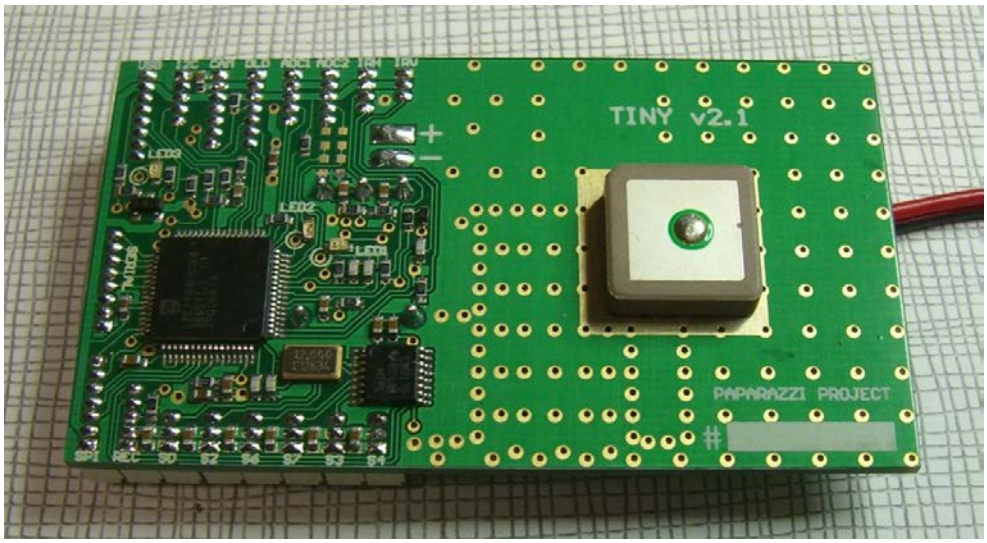

Figure 9.1: The Paparazzi Tiny v2.11.

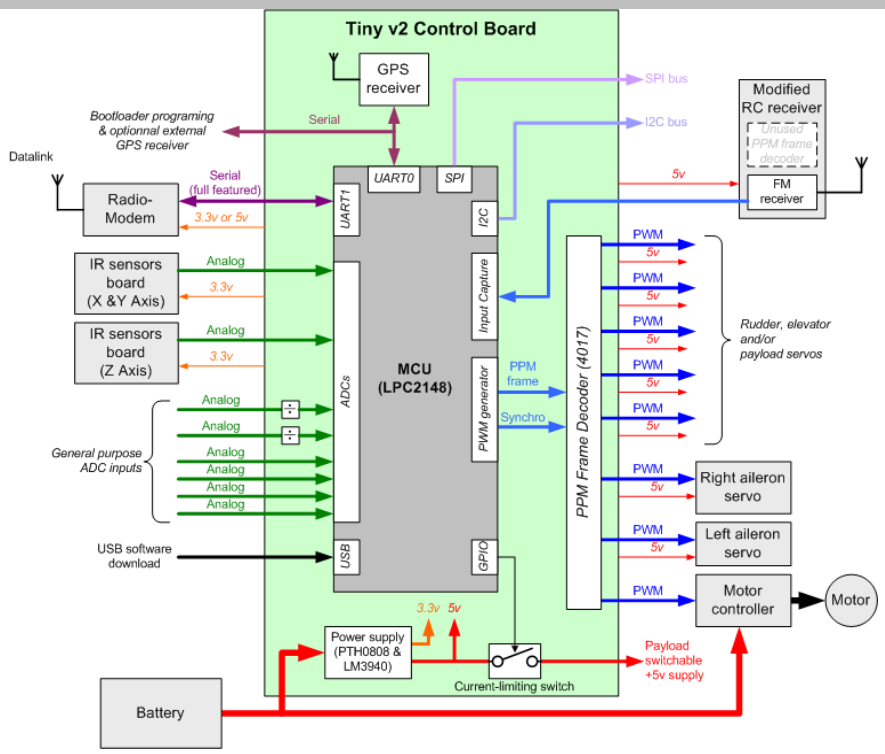

Figure 9.2: Paparazzi Tiny 2.11 System Architecture.

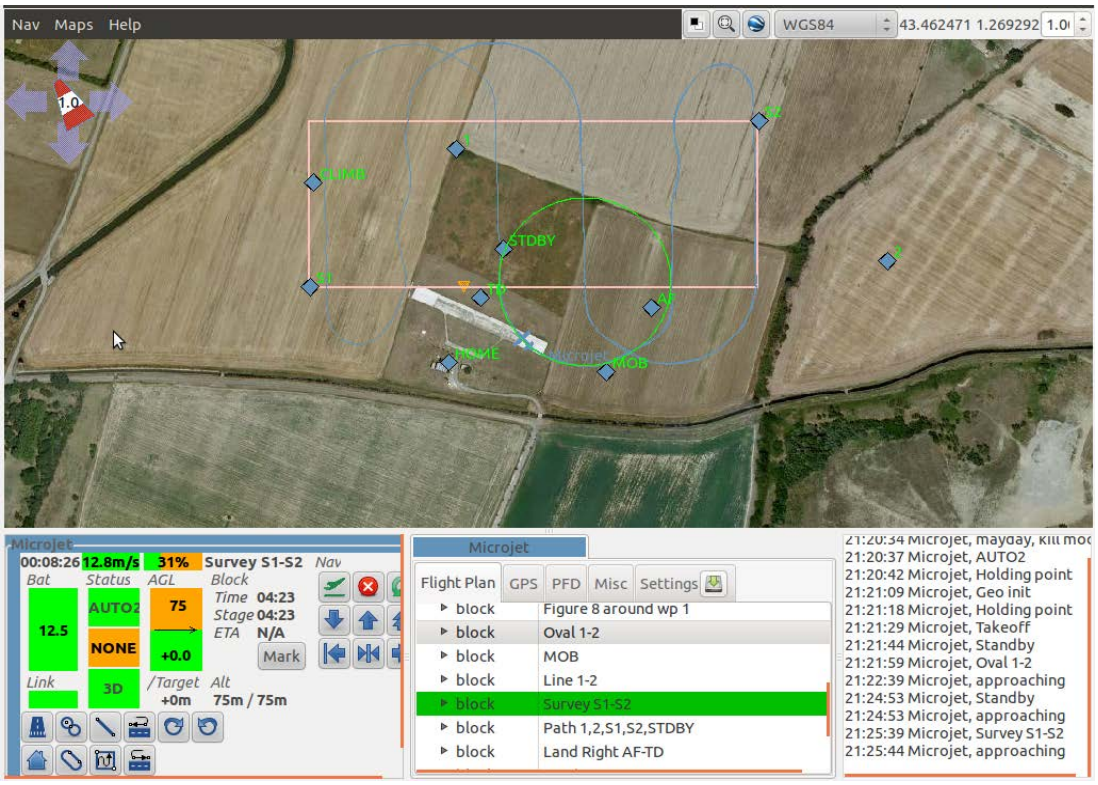

Figure 9.3: Paparazzi Tiny v2.11 Ground Control Station GUI.

9.2 Autopilot Sensors

The autopilot sensors are what supply the autopilot board and program with the flight data so the program can decide what to do. These are important because the autopilot program needs these to know how to control the servos going to the flaps of the SUAS. Some of the important sensors are the GPS, orientation sensor, and airspeed sensor. As mentioned before, the GPS needs to be accurate under 100ft and refresh at a rate no greater than 1Hz. The GPS also should have an easy interface to the autopilot board. This is very important when selecting a GPS Sensor. Power usage, size, and weight are also important as usual. The two GPS receivers that were selected the u-Blox LEA-4P receiver and the Navilock NL-507ETTL.

GPS Decision Matrix Criteria	weight		u-Blox LEA-4P Grade	Weighted G		Navilock NL-507 Grade	Weighted G
Power Usage	0.15		4	0.6		3	0.45
Size and Weight	0.1		4	0.4		3	0.3
Refresh Rate	0.2		4	0.8		3	0.6
Accuracy	0.3		4	1.2		4	1.2
Compatibility	0.25		5	1.25		3	0.75
Total	**1**		**21**	**4.25**		**16**	**3.3**

Table 9.2: GPS Decision Matrix with u-Blox LEA-4P and Navilock NL-507ETTL.

The LEA-4P came out to be the best selection to complete our mission objectives. It uses the least amount of power, and takes up a smaller amount of space at less weight. The major factor was the fact that the LEA-4P is built into the Paparazzi Tiny v2.11 autopilot board that was selected before. This makes configure the entire autopilot system much easier and lowers the chance of errors in the system.

Figure 9.4: u-Blox LEA-4P GPS

There are two basic ways to calculate the orientation of the SUAS. The first way is to use infrared sensors. The infrared sensors use the temperature of the earth and sky to calculate the how the aerial vehicle is oriented at any given time. The thermopiles are very sensitive which allows the difference to be seen. The temperatures are sent to the autopilot where the calculations are made. The other way is to use an inertial measurement unit (IMU). An IMU uses accelerometers and gyroscopes to calculate the orientation. Most IMU's do the calculations on board and then send the data to the autopilot board. The accuracy is the most important for measuring the orientation. If it is wrong, then the aerial vehicle will crash. The main disadvantage of the IMU is that it calculates the orientation based on previous measurements. So, errors in measurements are compounded with every measurement that is made. With the mission objectives having a flight time that could be an hour long, having compounding measurement error cannot happen. That is why infrared sensors were chosen.

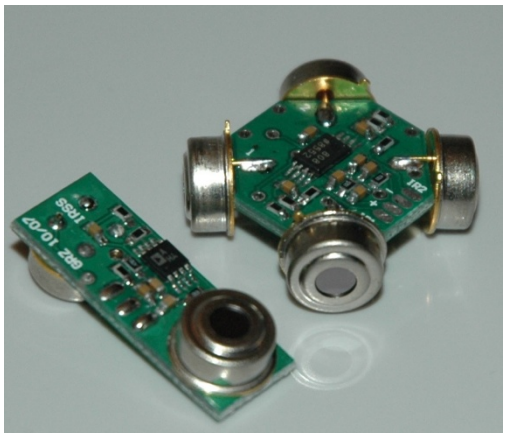

Figure 9.5: IR Vertical and Horizontal Sensors.

The last sensor to be picked is the airspeed sensor. Due to the autopilot board picked previously the only airspeed sensors supported are the airspeed sensor from Eagle Tree Sensors. The airspeed sensor will directly connect to the autopilot board using the I^2C connector on the board. The sensor will relay the raw data measured to the board so that the airspeed of the aerial vehicle can be more accurately be measured. With a more accurate airspeed, the autopilot board will be able to regulate the throttle better, leading to better power management.

9.3 Autopilot Communication

The autopilot data communication can be handled by several different types of modules. The 900MHz and 2.4GHz bands are public bands that anyone can use so the module being used would need to be in one of these bands. These bands would also be good for a fast data transfer. The modules would need to be small and power efficient and handle the range. Since the mission objectives do not state a maximum range handled, we predict that a range of 5 miles would be sufficient to complete the objectives. The modules would also need to interface with the autopilot board.

The R/C receiver that interfaces to the autopilot board is the main controls of the autopilot. The R/C receiver needs to be capable of complete manual control of the plane due to the mission requirements. The R/C interface also needs to have a switch that can tell the autopilot board to switch between manual mode and autonomy mode. Along with these important requirements the receiver needs to interface with the autopilot board and be efficient with space. The unit must also operate at a frequency that does not interfere with the camera system (2.4GHz) and autopilot data communication (900MHz).

With the Paparazzi Tiny v2.11 autopilot board being selected previously the best data communication modules will be the Xbee Pro 900 module. This module has a line of sight range up to 6 miles with a high gain antenna, data rate of 156 Kbps, and operates at 900MHz. The

module also has the interfacing software built into the autopilot board, making it easy to interface with the autopilot board

Figure 9.6: Xbee Pro 900 RF Module and Futaba 7CAP Transmitter.

The R/C unit being used is Futaba 7CAP transmitter and receiver. This combination is in the possession of the team and therefore the best option to use. The unit uses 7 channels and operates at 72MHz. The transmitter has all the necessary controls to be able to completely control the aerial vehicle and also has a three position switch that can be used to control the autonomy and manual modes for the autopilot. The autopilot program used uses an .xml file to configure the channel settings on the R/C receiver and therefore is very configurable for the Paparazzi Tiny v2.11.

10.0 Power Supply System Design

10.1 SUAS Electronic Components Requirements

To efficiently design a power supply system for the SUAS, the various components that make up the aircraft's complete electrical system must be individually analyzed. As is seen in fig 10.1, the components of the aircraft that will be supplied electrical power include the avionics system, the propulsion system and the image processing system.

In the Avionics system the main component is the Paparazzi autopilot board. This board has built a built in voltage regulation system which is utilized in the final power supply system design. In addition to the autopilot, servos and transmitter, there are several other important hardware components of the autopilot system that are separate from the physical board. These include infrared sensors, a GPS sensor and air speed sensors.

The propulsion system consists of a brushless DC motor along with an Electronic Speed Controller (ESC) and a Batter Eliminator Circuit (BEC). The purpose of the ESC is to allow the autopilot or human pilot to throttle the brushless DC motor effectively. The ESC also increases the efficiency of the motor output during cruise, and will protect the supplying batteries from being completely discharged. The BEC connects to the ESC and is a low loss voltage regulator that provides a constant voltage to all the servos on the aircraft.

The image processing system includes the camera, which does not contain its own dedicated batteries, the servos used to operate the gimbal and the image transmitter.

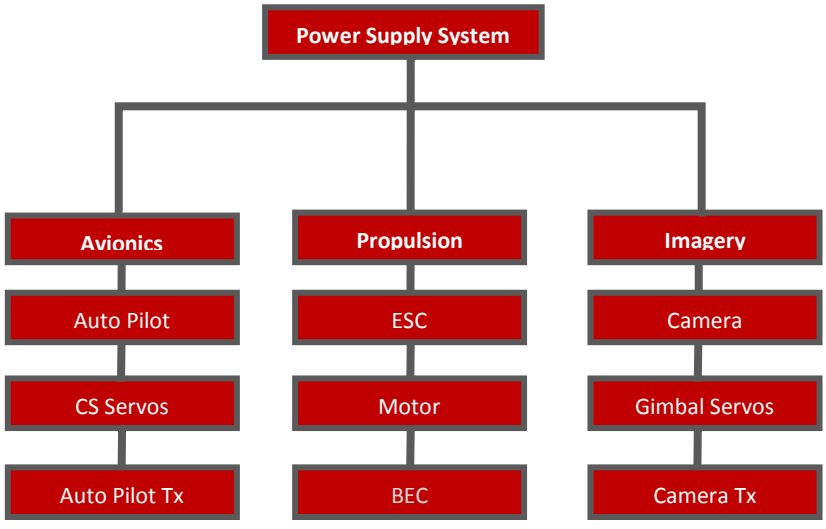

Figure 10.1: Power Supply Consumers

In order to design an effective power supply system, two important parameters must be determined for each electronic component. These two parameters are the required supply voltage, and the current consumption. Requiring the electronic components of the aircraft to operate for one hour provides a starting point with which the current consumption of the entire aircraft can be analyzed, which will determine the total current capacity of the power supply system. With these two parameters, the supplied voltage and current capacity, a power supply system can be designed which will meet the requirements of the aircraft.

10.2 Propulsion System Analysis

Analyzing the propulsion system starts with the propulsion requirements of the aircraft's mission; with respect to the aircraft weight and the mission profile. For an aircraft of 18 lbs, the required power for cruise was estimated to be 150 watts and the required power for takeoff was estimated to be 550 watts. The cruise estimation includes the search area maneuvers, and the power required for landing is considered negligible. These estimations were based on the requirements of a similar aircraft and are shown in figure 10.2.

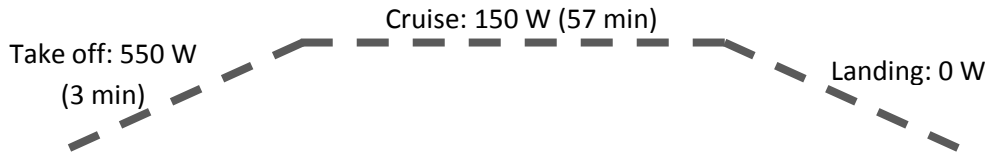

Figure 10.2: Mission power requirements profile

Based on the power requirements of the mission profile, a maximum output power of 550 W is used to select an appropriate brushless DC motor. The AXI 4130/20 Gold line brushless DC outrunner motor was selected based on several parameters. The output power, weight, battery cell requirement, cost and efficiency were used to select this specific motor. The decision matrix for the available brushless DC motors are shown in table 10.1. A grade of 1-5, was used in the decision matrix signifying a grade of poor (1), satisfactory (2), good (3), excellent (4) or outstanding (5). More weight was given to the required battery cells, as this increases battery weight dramatically. The power and efficiency of the motors are similar, so less weight was given to those score, while the cost of the motor was deemed of medium importance.

Motor Criteria	weight	AXI 5320/28 Grade	AXI 5320/28 Weighted G	Elite Power 60 Grade	Elite Power 60 Weighted G	AXI 4130/20 Grade	AXI 4130/20 Weighted G
Weight	0.2	2	0.4	4	0.8	3	0.6
Cell # (LiPo)	0.25	3	0.75	4	1	4	1
KV (RPM/V)	0.15	3	0.45	4	0.6	4	0.6
Max Power	0.1	4	0.4	3	0.3	4	0.4
Efficiency	0.1	5	0.5	4	0.4	4	0.4
Cost	0.2	3	0.6	3	0.6	4	0.8
Total	**1**	**20**	**3.1**	**22**	**3.7**	**23**	**3.8**

Table 10.1: Brushless DC motor decision matrix

As can be seen from table 10.1, the AXI 4130/20 was the better choice based on these parameters by only a slight margin. The selection of this motor was also based on the availability of this motor from vendors that could also supply other components of the aircraft, and better reviews from previous testing in RC aircraft. The specific characteristics of the AXI 4130/20 motor are shown below in table 10.2, and are used to analyze the power supply requirements of the propulsion system.

AXI 4130/20 Specifications	
Cell # (Lipo)	8
RPM/V	305
Max Efficiency	88%
No Load Current	1.2 A
Internal Resistance	99 mohm

Table 10.2: AXI 4130/20 Specifications

With these motor parameters, a graph can be draw showing the output power of the motor versus the input current from the power supply system. The supplied voltage is dependent on the type of battery and the number of cells used. For this graph, a LiPo battery is assumed, with the manufacturer recommended 8 cells. LiPo cells supply 3.7 V individually, so the recommended supply voltage to this motor is 29.6 volts. On graph 10.1, the two mission profile points are plotted. The first point (p1) is the required power for takeoff which will last approximately 3 minutes. The second point (p2) is the required power for cruise, which includes the search area maneuvers and will last approximately 57 minutes.

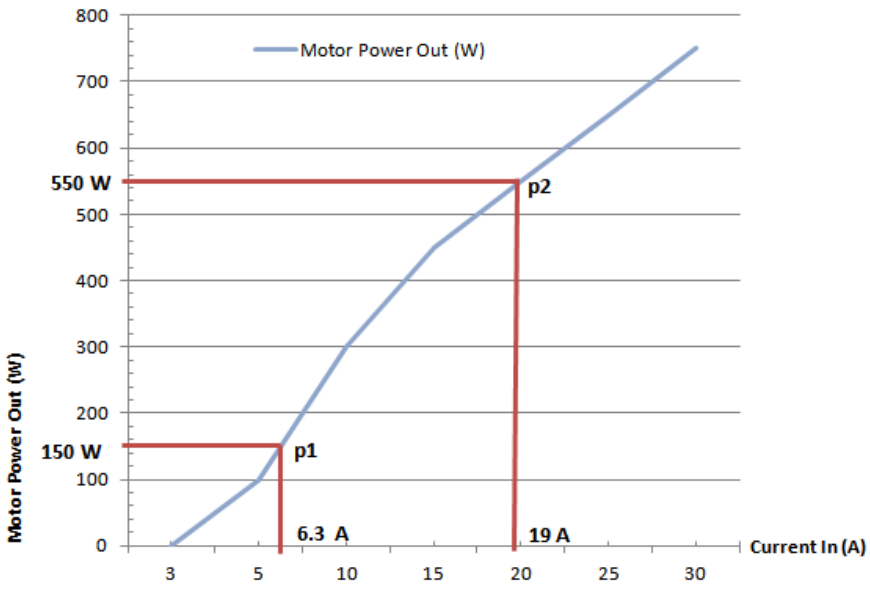

Graph 10.1: Motor Power output vs. Current Input for the AXI 4130/20

From this graph, which was developed using online software, the required current for cruise is determined to be approximately 6.3 A and the current required for takeoff is determined to be 19 A. The total current consumption of the motor for the entire mission can then be calculated as:

$$C_{tot}(t) = \sum I_{req} * t_{total} = (I_{cruise} * t_{cruise} + I_{takeoff} * t_{takeoff})$$

Where C_{tot} is the total current capacity required by the motor in Amp hours (Ah), calculated as the sum of the required currents multiplied by the respective times. For a capacity in Ah, the time is inputted in hours. The equation is then:

$$C_{tot}(t) = 6.3A * 0.95h + 19A * 0.05h = 6.935\ Ah$$

The Required current capacity for the motor for one hour of operation is therefore calculated as being 6.935 Ah.

10.3 Propeller Considerations

The propeller size for this particular motor is recommended by the manufacturer as 16" by 10". Because overloading the motor using an unsuitable propeller can damage the motor severely, a 16" diameter by 10" pitch propeller is selected and will be further tested in the lab when procured. An example propeller is shown in figure 10.3.

Figure 10.3: 16” by 10” Propeller

The remaining components of the propulsion system are the electric speed controller (ESC) and the battery eliminator circuit (BEC). The ESC controls the motor’s speed based on input from either the autopilot or a human interface control. It is used to throttle the motor for effective thrust during takeoff and efficient power output during flight. The Phoenix ICE 100 Brushless ESC was chosen as the best option for this propulsion system, based on its high voltage rating, onboard data logging capability, and its high efficiency rating. The BEC is used to regulate the 29.6 V supplied by the batteries into a voltage that can be used by the various servos on the aircraft. The BEC can be purchased separately, or can be integrated into the ESC based on the model. For the current design, the BEC is integrated into the ESC and will supply a regulated 5 V for the servos on the aircraft. The specifications for the selected ESC are shown below in table 6.3. The ESC will then be supplied 29.6 V, and is capable of supplying the motor with the required current range of 6.3 to 19 A. The power consumed by the ECS and BEC is caused mainly by the parasitic resistances of the component circuitry, and compared to the motor consumption, is estimated as approximately 0.7 mA.

Phoenix ICE 100 Specs	
Cell # (LiPo)	8
	34 V
Max Current Out	100 A
BEC Output	5-7 A
Weight	56.7 g

Table 10.3: ESC Specifications

The propulsion components are then as shown in table 10.4. Their respective current consumptions are calculated for a 60 min total flight time. The total current consumption of the propulsion system is calculated as 6.94 Ah. This calculation will be used to design the overall power supply system.

Propulsion Component	Supplied Voltage (V)	Current Consumption (mAh)
Phoenix 100 ESC	29.6	0.5
Intergrated BEC	29.6	0.2
AXI 4130/20 Motor	29.6	6935
		6935.7

Table 10.4: Propulsion System Electronic components

10.4 Avionics System Analysis

The Avionics system is the brains of the aircraft and contains the autopilot, the control surface servos, and the transmitter used for the autopilot/groundstation communications. The difficulty in analyzing the avionics system lies in the actual autopilot board, the Paparazzi Tiny V2. The board has multiple configurations, and can supply several different switching voltages to various components of the avionics system. The current consumption and supply voltage is then entirely dependent on the components used in the avionics system including the specific components used for navigation and orientation. The complete basic avionics system is shown below in figure 10.4. The navigation and orientation sensors include the GPS, vertical and horizontal sensors, and the airspeed sensor.

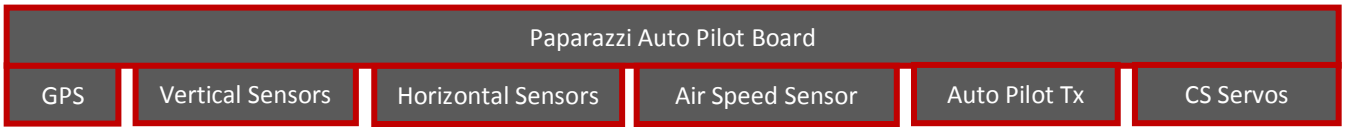

Figure 10.4: Basic avionics system overview

By estimating the individual supply voltage required and the current consumption of each component, the entire avionics system can be analyzed as a whole. The total current consumption for the avionics system can be calculated as:

$$C_{tot}(t) = \sum I_{Avionics} * t = \left(I_{autopilot} + I_{servos} + I_{Tx} + I_{sensors}\right) * t$$

Solving with estimated values and a t = 1 hour.

$$C_{tot}(t) = (.02 + .16 + .221 + .03) * 1 = \ .431Ah = 431\ mAh$$

The total current consumption is then calculated to be 431 mAh. The separate avionics components and their estimated power supply requirements are shown in table 8.5. The voltage supplied to the paparazzi board can be within a range of 6 to 18 V, however, because of the voltage range of the possible power supply design, the best voltage for the board is 11.1 V. The voltage supplied to the navigation and orientation sensors does not need to be taken in to account, as it is variable and is supplied through the Paparazzi board.

Avionics Components	Supplied Voltage (V)	Current Consumption (mAh)
Paparazzi Board	11.1	20
Nav/Ori Sensors	N/A	30
CS Servos	5	160
Xbee Transmitter	3.3	221
		431

Table 10.5: Avionics System Electronic Components

The total current consumption of the avionics system is calculated for a 60 min total flight as 431 mAh. This calculation will be used to design the overall power supply system.

10.5 Imagery System Analysis

The imagery system consists of a video camera, a gimbal system capable of housing and manipulating the camera, and a transmitter for feeding video to the ground station. The power supply system must then be able to supply the electronic components of this system, including the servos used to move the camera gimbal. The basic image processing system is shown below in figure 10.5.

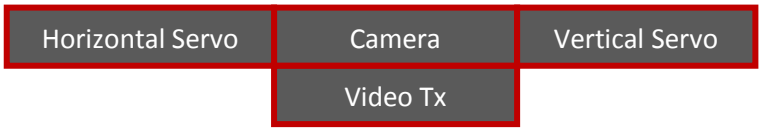

Figure 10.5: Basic imagery system overview

The required supply voltage and current capacity for this system is entirely based on the specified parameters of the individual components. After selecting the Sony FCB-IX11A block camera, the Lawmate 2.4GHz 1000mW 8Ch Wireless A/V Transmitter Module, and estimating the servo draw for 2 servos supplied 5 volts; the following information can be determined:

Imagery Components	Supplied Voltage (V)	Current Consumption (mAh)
Sony FCB-IX11A	11.1	200
Lawmate 2.4 GHz	N/A	500
Gimbal Servos	5	50
		750

Table 10.6: Imagery System Electronic Components

The total current consumption of the image processing system is calculated for a 60 min total flight as 750 mAh. This calculation will be used to design the overall power supply system.

10.6 Power Supply System Battery Analysis

By taking the calculated power consumption values for the avionics, propulsion and image processing systems, a power supply system can be designed to supply the systems in the most efficient manner possible. The power supply system components are the batteries, the voltage regulators required in the aircraft, and all the conductors carrying the required current to the loads. Other auxiliary components of the power supply system are the battery recharging and balancing devices, the ground station power supply system and any required electromagnetic Interference (EMI) shielding.

The most basic elements of this power supply system are the electrical storage devices, the batteries. Three different types of batteries were examined for this design, including Nickel Cadmium, Nickel Metal Hydride and Lithium Ion Polymer batteries. The Nickel Cadmium batteries were not considered for this design based on the environmental issues surrounding their disposal, and the obvious superiority of the two other battery types. The specific

characteristics of each type of battery are shown below in table 10.7. The two battery types considered were the Lithium Polymer and Nickel Metal Hydride batteries.

Battery Composition	Abbrev.	Specific Energy (Wh/kg)	Energy Density (Wh/L)	(Dis)Charge Eff.	Specific Power (W/kg)
Nickel-Cadmium	NiCad	40-60	50-150	80%	150
Nickel-Metal Hydride	NiMH	60-120	140-300	66%	250-1000
Lithium-Ion Polymer	LiPo	130-200	300	99.80%	7100

Table 10.7: Battery type characteristics

From table 10.7, it is evident that the Lithium Ion Polymer (LiPo) battery is far superior to the other types as far as capacity per weight and charge/discharge efficiency. The decision matrix for the tow considered batteries are shown in table 10.8. . A grade of 1-5, was used in the decision matrix signifying a grade of poor (1), satisfactory (2), good (3), excellent (4) or outstanding (5). More weight was given to parameters that are important for the design of aircraft; low weight, small size, low heat emission, and the ability to store and deliver the required electrical energy necessary for flight.

Battery Decision Matrix		NiMH Battery		LiPO Battery	
Criteria	weight	Grade	Weighted G	Grade	Weighted G
Performance	0.2	4	0.8	5	1
Weight	0.25	3	0.75	4	1
Size	0.25	1	0.25	5	1.25
Cost	0.1	5	0.5	1	0.1
Safety	0.2	5	1	3	0.6
Total	**1**	**18**	**3.3**	**18**	**3.95**

Table 10.8: Battery decision matrix

The LiPo battery was the choice battery mostly due to its low weight per capacity, small size, and high performance. The LiPo battery type was analyzed to insure that it was the best choice for this particular aircraft application. A unique feature of the LiPo battery is its discharge curve. As shown in graph 10.2, the voltage of the LiPo battery remains fairly linear until the individual cell voltage falls under the “critical voltage”. For most LiPo cells, this is approximately 3 volts. Over discharging of the LiPo cells damages the battery, and will decrease the lifespan of the battery pack. The ESC that will be connected to the motor and motor batteries will prevent this from happening, as it has a low voltage cut-off around 3 V. However, if any additional batteries are added to the power supply system, a low voltage cut-off device must be added to insure the batteries are not over discharged.

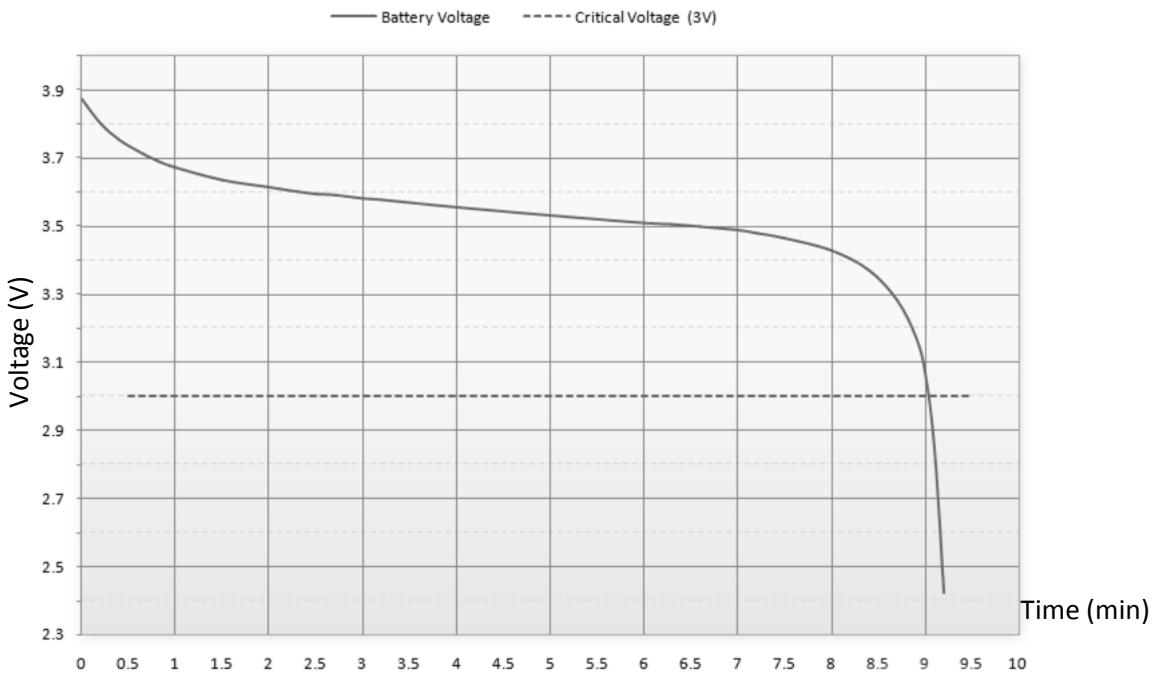

Graph 10.2: LiPo battery discharge curve (By Aaron Moore, 2008)

Another consideration when using LiPo batteries is the volatility of the chemicals used to manufacture the batteries. LiPo batteries can burst into flame or explode when the cells are damaged or punctured. Damage can also be caused to the battery from over charging or over discharging the cells, either of which may ruin the battery pack. Good practices that decrease the probability of LiPo battery damage include a pre-usage inspection, using a LiPo battery charger and never discharging a LiPo battery below a cell voltage of 3 volts.

Adding together all the required current capacities for the various aircraft, the total cuurent capacity required from the batteries can be calculated as:

$$C_{tot} = (C_{avionics} + C_{propulsion} + C_{Imagery})$$

Plugging in all the values:

$$C_{tot} = (431\ mAh + 6935.7mAh + 750\ mAh) = 8.12\ Ah$$

The total current capacity for the aircraft is calculated as 8.171 Ah. To simulate the LiPo battery performance in MatLab, an 8.5 Ah LiPo battery is connected to the three current drawing aircraft systems. Using Simulink, as shown in figure 10.6, the 8.5 Ah LiPo battery is simulated for 72 minutes. The battery's voltage, state of charge (SOC) current and power is shown in graph 10.3.

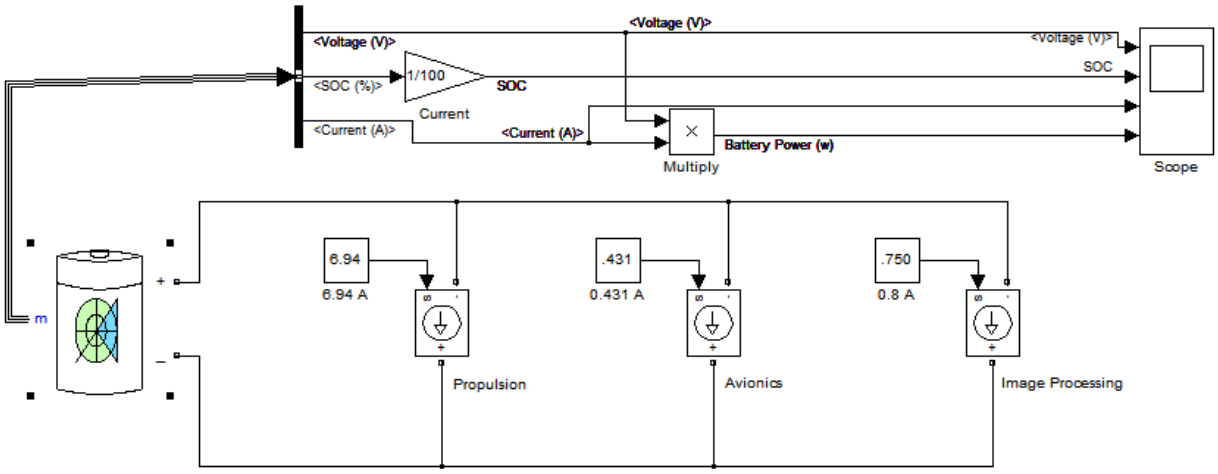

Figure 10.6: Simulink 8.5 Ah LiPo battery schematic

As was determined from the Simulink results, using at least 8.5 Ah of capacity of batteries will power the aircraft components through an hour of flight time without reaching the 3 V cutoff voltage of the ESC and low voltage cut off device. The simulation also shows that the voltage of the battery is at the required voltage for the motor and ESC for the majority of the flight until the completion of the mission and landing time. The battery supplied current is also shown to be steady, and the performance of the LiPo battery for this application is verified. It is important to note that over an hour of the SUAS simulated function; the battery voltage does not fall below 4 volts. This is a validation of an 8.5 Ah battery being sufficient to supply the SUAS over the mission time without being over discharged.

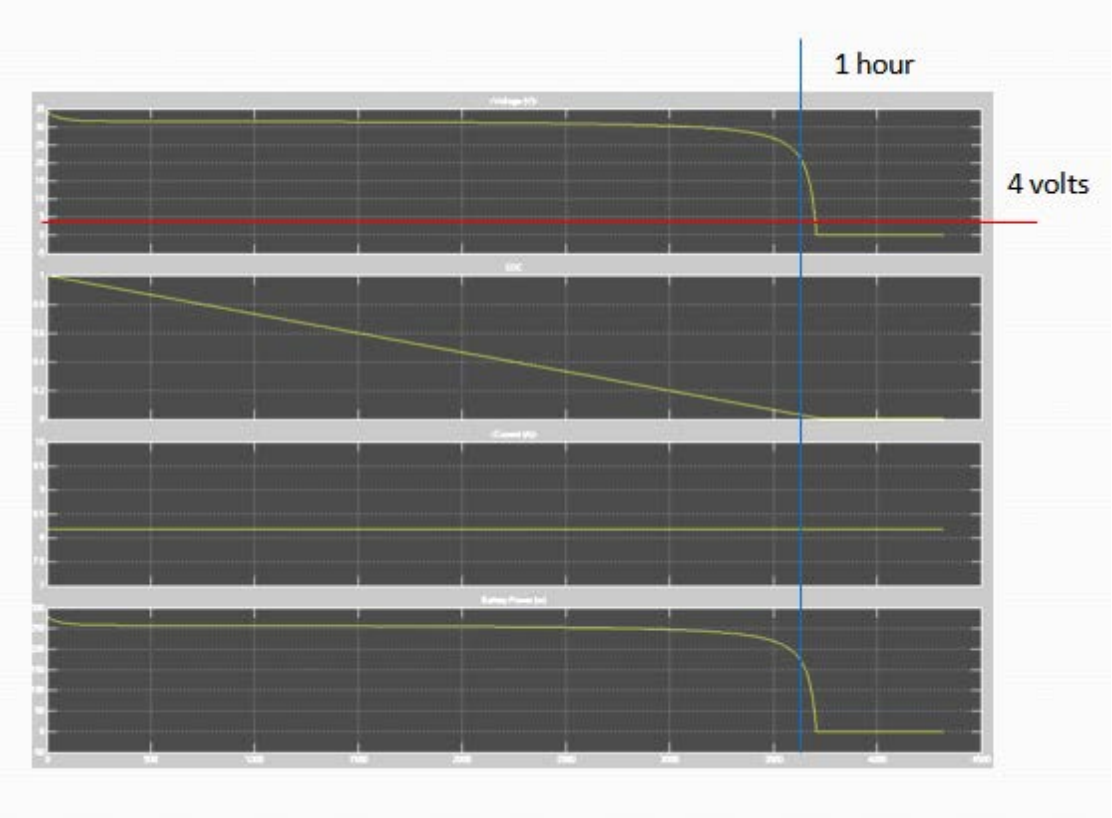

Graph 10.3: Simulink 8.5 Ah LiPo battery simulation results

10.7 Complete Power System Design

With the required battery capacity of at least 8.5 Ah, the entire aircraft electronics system can be analyzed and the total power supply system designed. The aircraft electronic components with their required supply voltages and currents are shown in table 10.9. The components can be grouped according to supply voltage into four different voltage zones.

Component	Required Voltage (V)	Supplied Voltage (V)	Voltage Zone
BEC	29.6	29.6	1
Motor ESC	29.6	29.6	1
AXI 4130/20 Motor	29.6	29.6	1
CS Servos	3-6	5	2
Gimbal Servos	3-6	5	2
Paparazzi Board (Complete)	6-18	11.1	3
CCD Block Camera	6-12	11.1	3
Lawmate Video Tx	10.5-13	11.1	3
Xbee Tx	3-3.6	3.3	4

Table 10.9: Aircraft electronic components specs and voltage zones

With the voltage zones being so far apart it is necessary to either use multiple voltage regulators, or separate batteries for the two main voltage zones. By using an 8-cell LiPo battery, the required voltage of 29.6 volts can be supplied to the components in zone 1. The 11.1 volt supply voltage of zone 3 could be supplied by using a 3-cell LiPo battery. The integrated BEC in the Phoenix ICE 100 Brushless ESC is capable of regulating the 29.6 volts from the zone 1 battery to the 5 volts required for voltage zone 3. The final zone, zone 3, can be supplied by the zone 3 battery and regulated to 3.3 volts through the Paparazzi onboard regulator. The voltage zones and their suppliers are shown in table 10.10. The total current capacity for each zone supplier was calculated using the values of current consumption from table 10.9.

Zone	Supplier	Voltage (V)	Total Required Capacity (mAh)
1	[2] 8-Cell LiPos (7700mAh)	29.6	7145.7
2	ESC Integrated BEC	29.6	N/A
3	[1] 3-Cell LiPo (1300 mAh)	29.6	971
4	Paparazzi Board	5	N/A
			8116.7

Table 10.10: voltage zones and suppliers

From table 10.10, the appropriate 8-cell LiPo battery should have a capacity of at least 7145.7 mAh and the 3-cell battery should have a capacity of at least 950 mAh. The two selected battery designs are to use two 8-cell 3850 mAh LiPo batteries in parallel to supply voltage zone 1. With these two batteries in parallel, the supplied voltage will be 29.7 V and the total capacity will be 7700 mAh. Voltage zone 3 will be supplied with a single 3-cell 1300 mAh LiPo battery. The single battery will supply zone 3 with 11.1 volts and will supply up to 1300 mAh. The two battery types selected are both manufactured by Thunder Power and are specifically designed for RC airplane applications. Selecting batteries with capacities higher than what is required allows for more a larger operating window time wise and decreases the possibility that the batteries will be overly discharged. The total top-level electronics design for this aircraft is shown in figure 6. The power supply system connections are shown, as well as the various communications connections. The independent battery tests are shown in graph 10.4.

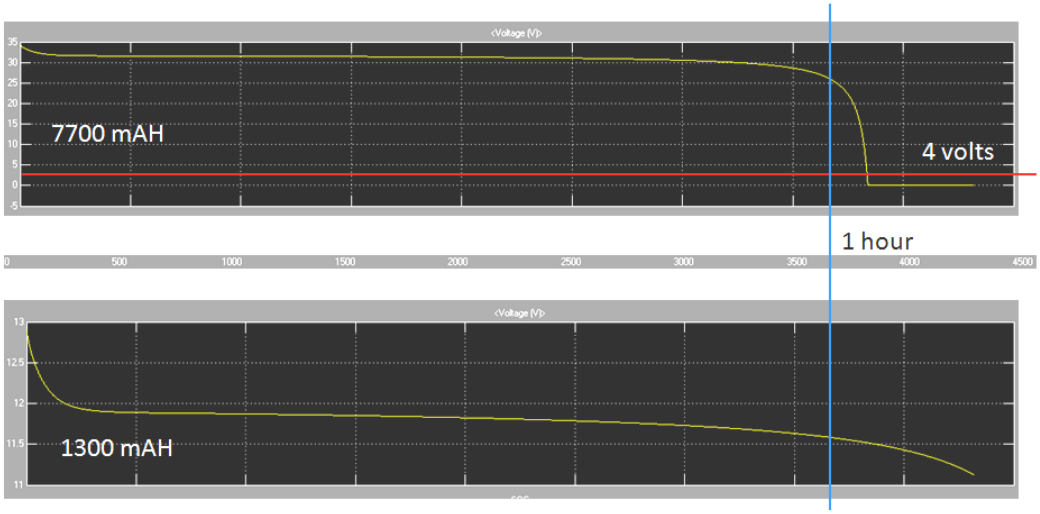

Graph 10.4: Simulink Independent LiPo battery simulation results

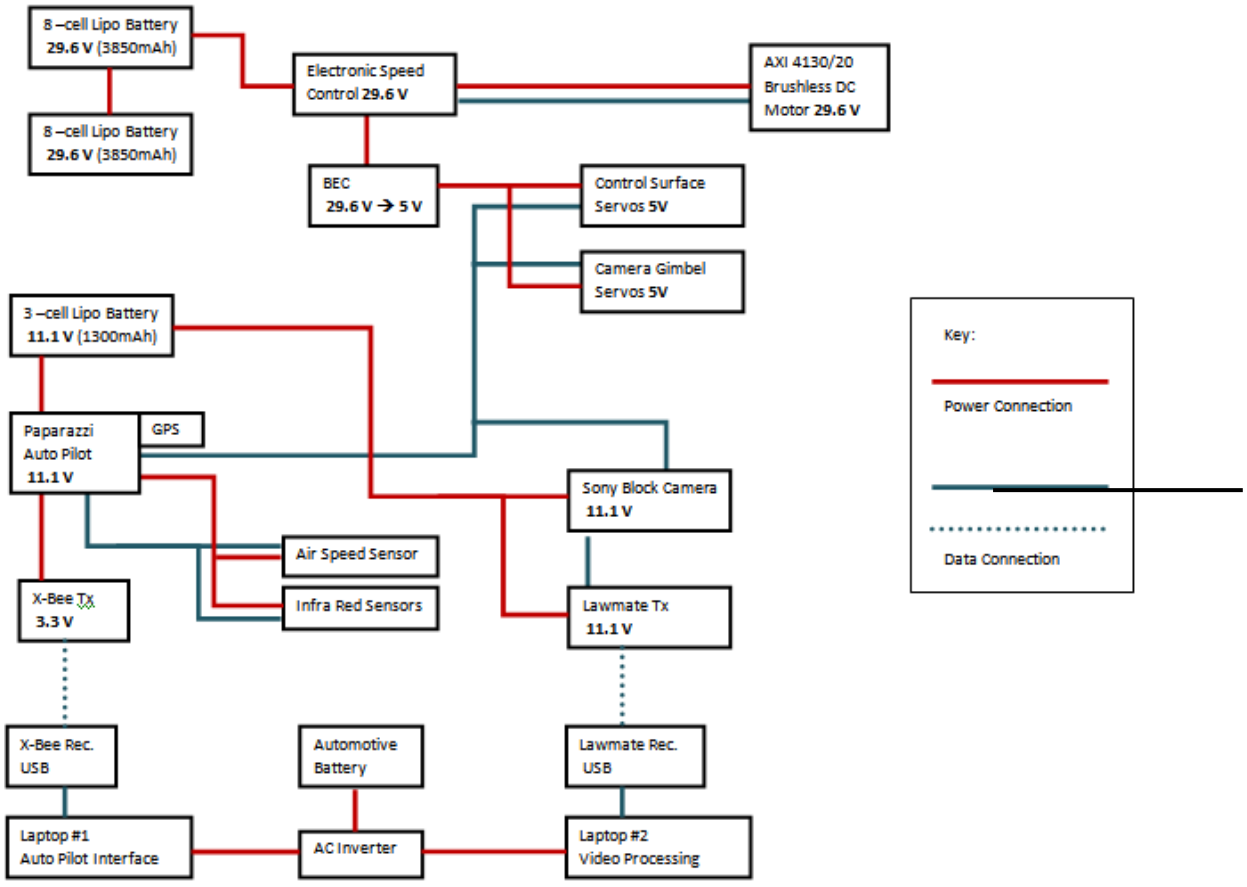

Figure 10.7: Top-level aircraft electronics diagram

11.0 Auxiliary Design Sections

11.1 The Ground Station

The ground station is a vital communications link to the airborne UAV. It is necessary that the data sent from the autopilot and video systems are received quickly and clearly. The ground station components include an aircraft remote control transmitter, the Paparazzi GUI, an imaging system video receiver, the image processing system and a power supply. A possible component layout is shown in figure 11.1. Due to the remote operating locations of the UAV the ground station may be optionally powered from a lead acid deep-cycle battery. The battery directly connects to a DC-AC converter which allows NEMA 5-15 (standard North American wall outlet connection). This solution is definitely not the most efficient way to provide power to the ground station, but is cheap and easily available. Another solution is to use a small generator that provides enough power for roughly an hour of flight time.

Figure 11.1: basic Ground Station Set-Up

11.2 The Camera Gimbal

The gimbal will be mounted to one of the spares inside the plane. It will hang below the plane. Its structure involves two servos. The servo mounted to the top of the gimbal will spin a gear and pinion. This will turn the entire structure about the axis in which the shaft at the top of gimbal. The servo mounted to the side of the gimbal will spin the structure holding the camera about the horizontal axis of the gimbal. The importance of the gimbal is to reduce the budget because the cameras with the built in gimbal costs were out of our range.

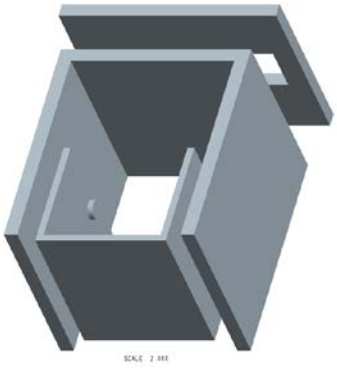

Figure 11.2: Camera Gimbal Pro-E Drawing

12.0 Safety and Environmental Considerations

12.1 Safety

Safety is always a top priority for the team. We want to make sure that during the process of engineering our aerial vehicle no person, objects, or the environment is harmed or damaged. There are several different steps to take to make sure that this doesn't happen. During the process, some hazardous items are the batteries and the plane itself.

The Lithium polymer batteries that are being utilized in the power supply system of the SUAS have a high discharge rate and a high current capacity per weight, but precautions must be taken to ensure that the batteries are being used in a safe manner. The lithium ions in these battery packs are held in a polymer matrix, and if the battery packs are punctured of damaged the battery chemicals can ignite and vent from the battery packaging. As shown in figure 7 the ignition of our battery packs would destroy the SUAS and its expensive components. Therefore, the following steps must be taken to avoid a battery fire.

1. The batteries will only be charged with their particular approved charger.

2. The cell count must be set correctly on the charger. (8 and 3 cells)

3. The cell voltages must be checked and balanced at the first usage of the batteries and before each run of the aircraft.

4. The batteries will never be left unattended while charging. Batteries should be removed from the SUAS prior to charging if possible.

5. Batteries should be charged at less than the max C value. (30C)

6. Batteries should be checked for ballooning during and after charging. Ballooned batteries should be discharged with a simple light bulb and disposed of.

8. If the aircraft crashes, the batteries should be immediately removed and placed in a non-flammable are such as pavement or a sand bucket.

9. Batteries should be charged in an open area away from personnel. In the unlikely chance that the batteries explode, dangerous fumes and material may be expelled from the batteries.

10. A fire extinguisher should be onsite at all times.

Figure 12.1: LiPo Battery Explosion

If the team loses control of the aerial vehicle, it can become like a missile. Safety measures have been taken to have the best chance of this not happening. The first lies in the autopilot software. The autopilot software chosen has a built in “return home” function. The aerial vehicle will return to the waypoint called home if it loses its telemetry connection. This keeps the plane from flying off from the chosen area into a dangerous zone. Another safety measure is in the R/C system. There is a kill switch on the R/C transmitter that allows a user to regain full control of the aerial vehicle if there were a need to do so. The user can steer the aerial vehicle into a safe location if the aerial vehicle travels to an unsafe location.

12.2 Environmental Considerations

Lithium Polymer batteries are being used for this project. While they are very efficient, they can be very harmful to the environment. The steps taken to make sure the lowest possible chance of something dangerous to happen is to have them securely connected to the plane and cover them in bright orange material. The bright orange material is so that if the batteries do become separated from the plane during flight, they can be more easily recovered by a search team. The actual manufacturing process of the batteries is also quite harmful to the environment, and there is currently not a recycling program in place for these batteries. However, by taking good care of the batteries we but, we can extend their lifetime and minimize any damage to the environment the buying additional batteries may cause.

The materials inside of the plane, aside from the balsa and plywood segments of the fuselage structure, are unfortunately hard to recycle but pose no immediate environmental concerns. Reinforced plastics can be recycled but the method used, grinding the matrix and reinforcement into a fine mixture and then using that as a later reinforcement product is rarely seen and no large scale recycling operations are currently active. If left in the environment they will keep their structure till they are either heated to a temperature of 350oF or worn by weather effects. They do not however produce any harmful byproducts.

During construction of the plane all members working on sanding the FRPs must wear masks or re-breathers to stop harmful dust from being inhaled. Masks must also be worn during applications of release agents in the molding process. Aside from these times there is no danger to the team in the production of the plane.

12.3 Failure Mode Analysis

Risk	Consequence	Remedy
Aircraft structural damage	The aircraft must be quickly repaired to proceed with testing. Major setbacks in scheduling or failure to complete final design depending on the severity of the structural damage due to manufacturing damage or crash landing.	Any damage must be repaired by May 2012 in order to comply with competition deadlines. The aircraft is to be designed in a modular way such that individual sections can be removed and repaired if necessary.
Autopilot systems failure	Aircraft may be recoverable with manual override in the event of autopilot failure. Although, if the autopilot cannot transmit PWM signals the aircraft will not be recoverable.	The autopilot system is the heart of the avionics system controlling the planes servos as well as the navigation sensors. Performing ground based tests before testing flight worthiness may prevent this from

		occurring. Another solution is to allow the Futaba 7cap transmitter to interface with the servos without passing through the Paparazzi board.
Power and Motor failure	Fairly unlike to be recoverable, the aircraft could be landed without power or sustain a small crash within extremely low altitudes. At operating altitudes this would result in major catastrophic damage. In the likelihood of a catastrophic crash, the aircraft may present hazardous environmental conditions due to the volatility of the battery payload.	Power failure would not allow the servos to control the direction of the plane. Therefore rendering it unguided and uncontrollable. Verifying full charge levels of the Lithium Polymer batteries may prevent this. The motor as well as the electronics should be tested thoroughly before attempting flight mission tests. A potential full power loss at high altitudes could potentially destroy all major aircraft components.
Imagery systems failure	Inability to distinguish targets from the air. Inexperienced pilots flying in manual mode could result in a crash without visual guide.	Safely land plane and verify there is no damage to the device. Connect the camera to the PC's serial port and attempt to operate the device. Structural damage to the lens or internal electronics may be un-repairable. A backup cheaper test camera will be used during early flight tests.
Communication systems failure	Major loss of signal to the autopilot would result a sudden loss of altitude. If the signal remains lost the aircraft will crash.	The three communication links will be ground tested in multiple locations before experiencing flight. Many of the communication components are commercially available off the shelf and can be repurchased if destroyed if budget permits.
Ground station failure	Loss of communication with the UAV will result in the aircraft returning home and flying above the designated home waypoint. Targets will no longer be identifiable with loss of	The ground station can be powered remotely by two methods, either a Lead-Acid deep-cycle battery with DC-AC inverter, or a gas powered Honda generator. Having both

	power.	systems available allows a backup in the event of one system failing during the competition.
Ordered parts become unavailable, arrive late, or are become backordered	Major schedule setbacks. Change of design or budgeting loss. Worst case scenario the project is not completed.	Selecting a group member to take care of all design purchases ensures a systematic track record of all expenditures. Ordering from reliable manufactures is a necessity. If necessary the design will be changed to work around unavailable components.
Lack of personnel	Significantly larger workloads for other group members. Setbacks in manufacturing and testing time. Worst case scenario the project remains incomplete.	Biweekly group meetings and other forms of communication ensure members of ME and ECE teams remain involved in the program as well as participating in design work. In the event a loss of personnel the design team could ask for help from graduate students or underclassmen to assist in the fabrication and testing procedures leading up to the competition.
School projects or holidays conflict with aircraft design schedule	Loss of time and schedule setbacks back incur. Group members may be unable to work during specific days/times due to other class requirements and require the group to be behind.	Several group members have decided to commit extra time outside of school, during holidays, to assist in the design and construction of the UAV. Any conflicts with meets and group related work days should be addressed ahead of time through the Team Leader or Secretary.
Insignificant budget	The project may be cancelled or left incomplete. The design may underperform its original plans due to less expensive construction materials or electronic components.	Financial budgets have been a concern throughout the project. The UAV project is directly funded by FCAAP and has been confirmed that the original budget may be increased to meet the design project needs.

12.4 Risk Assement

Ranking	Hazard Severity	Assessment Description
1	Minor	A negligible amount of damage with small or no personal injury. Aircraft and components are easily repairable with small rather insignificant first aid requirements.
2	Moderate	Slightly more significant damage to the aircraft and/or needed first aid assistance. The aircraft remains in a mend able state with no critical personnel injury.
3	Major	The aircraft experiences a rather large amount of damage such that the aircraft will not fly. The damage may be repairable but not in the immediate future, The personnel injury is significant with necessary assisted medical attention. Major personnel injury could be experienced in the event of a crash.
4	Critical	Damage to the aircraft renders it completely unusable. Some of the payload components survived and may be reused. Such a crash could result in serious personnel injury at high speeds with considerable environmental concerns from toxic batteries. Anyone harmed by the aircraft will need immediate medical attention as well as hospitalized care.
5	Catastrophic	In the event of a catastrophic disaster the aircraft could become a missile resulting in the destruction of the aircraft itself as well as endangering the lives of many individuals. This incident would involve personal exposure to highly flammable volatile batteries.

Ranking	**Probability**	**Frequency**
1	Extremely Unlikely	Never
2	Uncommon	Once or twice in the past
3	Sporadic	Monthly
4	Common	Weekly
5	Typical	Multiple times a week

Risk Assessment Matrix

Hazard Severity	Frequency 1 Extremely Unlikely	2 Uncommon	3 Sporadic	4 Common	5 Typical
Minor					
Moderate					
Major					
Critical					
Catastrophic					

Acceptable Task/Action

Semi-Acceptable Action

Unacceptable Action

Acknowledgements

The members of Senior Design Team #14 would like to thank our advisors Dr. Rajan Kumar and Dr. Mike Frank for their invaluable guidance during this semester. We would also like to express our gratitude to our families and significant others for the support they gave us over the semester.

References

1. Anderson, Chris. *DIY Drones*. Web. 04 Dec. 2011. <http://diydrones.com/>.
2. "Eagle Tree –R/C RPV RC Unmanned Aerial Vehicle Telemetry" *Eagle Tree – R/C Telemetry OSD RC Pitot Prandtl Spektrum AR9000 JR R921*. Web. 04 Dec. 2011. <http://www.eagletreesystems.com/Standalone/standalone.htm>.
3. Faludi, Robert. "XBee-PRO® 900 RF Modules - Digi International." *Making Wireless M2M Easy - Digi International*. Digi Internation Inc. Web. 05 Dec. 2011. <http://www.digi.com/products/wireless-wired-embedded-solutions/zigbee-rf-modules/point-multipoint-rfmodules/xbee-pro-900>.
4. "Futaba 7CAP." *RC Universe Features Rc Cars, Rc Airplanes, Rc Helicopters, Rc Electric Planes, Rc Boats, Radio Control Jets, Rc Discussion Forums, Rc Classifieds and Auctions.* Web. 05 Dec. 2011. <http://www.rcuniverse.com/magazine/article_display.cfm?article_id=321>.
5. "Main Page - Paparazzi." *Paparazzi*. GNU Free Documentation. Web. 04 Dec. 2011. <http://paparazzi.enac.fr/wiki/Main_Page>.
6. "Lithium-ion polymer battery" *Wikipedia* Web. 04 Dec. 2011. <http://en.wikipedia.org/wiki/Lithium-ion_polymer_battery>.
7. "LiPo battery guide" *prototalk.net* Web. 04 Dec. 2011. <http://exoaviation.webs.com/pdf_files/Lipo%20Battery%20Guide.pdf>.
8. "LiPo safety warnings" *Thunderpower* Web. 04 Dec. 2011. <http://thunderpowerrc.com/PDF/THPSafetyWarnings.pdf>.
9. Raymer, Daniel P. *Aircraft Design: a Conceptual Approach*. Reston, VA: American Institute of Aeronautics and Astronautics, 2006. Print.
10. Lennon, Andy. *Basics of R/C Model Aircraft Design: Practical Techniques for Building Better Models*. Wilton, CT: Air Age, 1996. Print.
11. Simons, Martin. *Model Aircraft Aerodynamics*. Poole, Dorset [England: Special Interest Model, 2002. Print.
12. "XFLR5." *Http://sourceforge.net/*. Web. 8 Dec. 2011. <http://xflr5.sourceforge.net/>.
13. "NACA-4412" Airfoil Investigation Database. Web. 8 Dec. 2011. <http://www.worldofkrauss.com/foils/793>
14. "NACA-0012" Airfoil Investigation Database. Web. 8 Dec. 2011. < http://www.worldofkrauss.com/foils/1137>
15. Gray, P. (2001). *Lines of resolution*. Web. 01 Dec. 2011. <http://jkor.com/peter/tvlines.html>
16. Hickman, I. (1997). *Practical RF Handbook*. Butterworth-Heinemann. Text. 01 Dec. 2011.
17. McHugh, S. (ND). *Digital camera image noise*. Web. 01 Dec. 2011. <http://www.cambridgeincolour.com/tutorials/noise.htm>
18. Antenna Basics. *Welcome to the Antenna Theory Website*. Web. 01 Dec. 2011. <http://www.antenna-theory.com>

19. Space-Electronics (ND). *How to reduce jitter of airborne cameras*. Web. 01 Dec. 2011. <http://www.space-electronics.com/KnowHow/Reduce_camera_jitter.php>

20. Sputnik-Inc (2004). *Rf propagation basics*. Web. 01 Dec. 2011. <http:///www.sputnik.com/docs/rf_propagation_basics.pdf>

21. Zuech, N. (2007). *Analog vs digital cameras - what is being used in machine vision*. Web. 01 Dec. 2011. <http://www.machinevisiononline.org/public/articles/archivedetails.cfm?id=1528>

22. Schafer, Marlon K. *How to Pick the Right Antenna*. www.electro-comm.com, 2001. Web. 1 Dec. 2011. <http://www.odessaoffice.com/wireless/antenna/how_to_pick_the_right_antenna.htm>

22. FCB-IX Series Datasheet. Park Ridge, NJ: Sony Electronics Inc, 2005. PDF.

23. Olson, Jenna, Kelly Garcia, Mark Zanmiller, and Doug Miley. *CCT Product List*. Cloud Cap Technologies - Goodrich ISR Systems, 12 Jan. 2011. PDF.

24. Struzak, Ryszard. "Basic Antenna Theory." Lecture. *School on Wireless Networking*. ICTP-ITU-URSI School on Wireless Networking for Development The Abdus Salam International Centre for Theoretical Physics ICTP, 2007. Web. 1 Dec. 2011. <http://wirelessu.org/uploads/units/2008/08/12/39/5Anten_theor_basics.pdf>.

Appendix A: Team #14 Documents

A.1 Team # 14 Code of Conduct

Mission Statement:

The objective of this team is to work together to create a positive and professional learning environment. This will be established through trust, respect, integrity and communication. We will work in a timely manner but also carefully to ensure that the project is done properly.

Team Officer Positions:

Team Leader: Ryan Jantzen

The Team leader is responsible for setting reasonable goals and managing project completion. Assures that workload is distributed evenly between the team members. Schedules team meetings and informs team of meeting time and place. Team Leader resolves conflicts within the team and sets meeting agendas.

Secretary: Alek Hoffman

The Secretary maintains and submits minutes for each team meeting and publishes all important documents, websites, ect. to the group blog. Secretary maintains rules and regulations for the team and project and alerts team mates of upcoming academic assignments and milestones.

Treasurer: Antwon Blackmon

The Treasurer is responsible for the group's finances as well as keeping track of purchased parts and overall inventory. Treasurer asses required expenses and plans for appropriate funding.

Webmaster: Brian Roney

The Webmaster is responsible for maintaining the team's project website with up to date information and media. Webmaster will research and share important online information with his team mates.

ME Lead: Walker Carr

The Mechanical Engineering Lead is responsible for managing ME members of team and scheduling meetings with the ME advisor. ME Lead will manage overall ME project requirements with the team leader and will keep in constant contact with ECE lead to ensure project compatibility.

ECE Lead: Eric Prast

The Electrical/Computer Engineering Lead is responsible for managing ECE members of team and scheduling meetings with the ECE advisor. ECE Lead will manage overall ECE project requirements with the team leader and will keep in constant contact with ME lead to ensure project compatibility.

Communication:

The primary sources of communication between team members will be through emails, phone calls, and text messages. An account for Google Calendar was set up to track meeting times and schedule deadlines for deliverables.

Meetings:

Meetings have been established twice a week; Tuesdays at 6pm and Fridays at 2pm. All members are expected to attend both meetings and missing these meetings without a valid excuse will not be tolerated. If a team member must miss a scheduled meeting, they must notify the entire team of their absence at least 24 hours in advance. An Evernote Notebook account was created for the secretary to record meeting minutes and distribute them to all team members.

Conflict Resolution:

In the event that a conflict should occur the following steps should be taken:

- The individuals involved should try and come to some sort of an understanding either agree or agree to disagree.
- If the individuals involved cannot come to an agreement then the conflict some be discussed with the rest of the group.
- The conflict should be explained in a clear manor to the rest of the group then a vote should be taken.
- If the vote ends in a draw then the team leader should make a decision.
- If the team leader cannot come to a conclusion then the conflict should be resolved by some outside source such as the faculty advisor

Ethics:

The team will follow the Codes of Ethics and Standards established by the American Society of Mechanical Engineers.

As a team we have all read and understand the code of conduct described above and plan to abide by it.

Antwon Blackmon _____

Walker Carr _____

Alek Hoffman _____

Ryan Jantzen _____

Eric Prast _____

Brian Roney _____

Team 14 Gannt Chart

Completion • Current Week 12

#	Activity	Begins	Ends	Planned Start	Dur	% Done
	Management					
1	Project Management	11-Sep-11	11-Jun-12	1	40	12%
2	NAPS	11-Sep-11	29-Sep-11	1	2	100%
3	Project Specifications	30-Sep-11	13-Oct-11	3	3	100%
4	CDR Presentation	14-Oct-11	27-Oct-11	6	2	100%
5	IDR Presentation	28-Oct-11	17-Nov-11	7	4	100%
6	FDR Presentation	18-Nov-11	8-Dec-11	11	3	50%
	Research					
7	Blanket Research	11-Sep-11	2-Oct-11	1	3	100%
8	Specified Research	3-Oct-11	16-Oct-11	4	2	50%
9	Design Research	10-Oct-11	7-Nov-11	6	4	100%
10	Structure Research	11-Sep-11	16-Oct-11	1	5	100%
11	Propulsion Research	11-Sep-11	16-Oct-11	1	5	100%
12	Materials Research	11-Sep-11	16-Oct-11	1	5	100%
13	Power Research	11-Sep-11	16-Oct-11	1	5	100%
14	Controller Research	11-Sep-11	16-Oct-11	1	5	100%
15	Sensor Research	11-Sep-11	16-Oct-11	1	5	100%
	Design					
16	Concept Generation	11-Oct-11	16-Oct-11	5	1	100%
17	Concept Selection	17-Oct-11	23-Oct-11	6	1	100%
18	Design Refinement	24-Oct-11	6-Nov-11	7	3	100%
19	Final Design	7-Nov-11	5-Dec-11	10	4	75%
20	Structure Design	17-Oct-11	4-Dec-11	6	7	100%
21	Propulsion Design	17-Oct-11	4-Dec-11	6	7	100%
22	Materials Design	17-Oct-11	4-Dec-11	6	7	100%
23	Power Design	17-Oct-11	4-Dec-11	6	7	100%
24	Controller Design	17-Oct-11	4-Dec-11	6	7	100%
25	Sensor Design	17-Oct-11	4-Dec-11	6	7	100%
	Prototype					
26	Part Ordering	12-Dec-11	31-Dec-11	14	3	0%
27	Initial Testing	2-Jan-12	22-Jan-12	17	4	0%
28	Intermediate Testing	23-Jan-12	19-Feb-12	21	4	0%
29	Final Testing	20-Feb-12	31-Mar-12	25	6	0%
30	Final Prototype	2-Apr-12	10-Jun-12	31	7	0%
	Competition					
31	Application	12-Dec-11	8-Jan-12	14	4	0%
32	Clearance	2-Apr-12	2-May-12	30	4	0%
33	Journal	1-May-12	24-May-12	34	4	0%
34	Compete	13-Jun-12	17-Jun-12	38	3	0%
35				0	0	0%

Week: 1 2 3 4 5 6 7 8 9 10 11 12 13 14 15 16 17 18 19 20 21 22 23 24 25 26 27 28 29 30 31 32 33 34 35 36 37 38 39 40

Planned

A.2 Team #14 Gannt Chart

Appendix **B**: **Electronic Design Diagrams**

B.1 Imagery System Detail

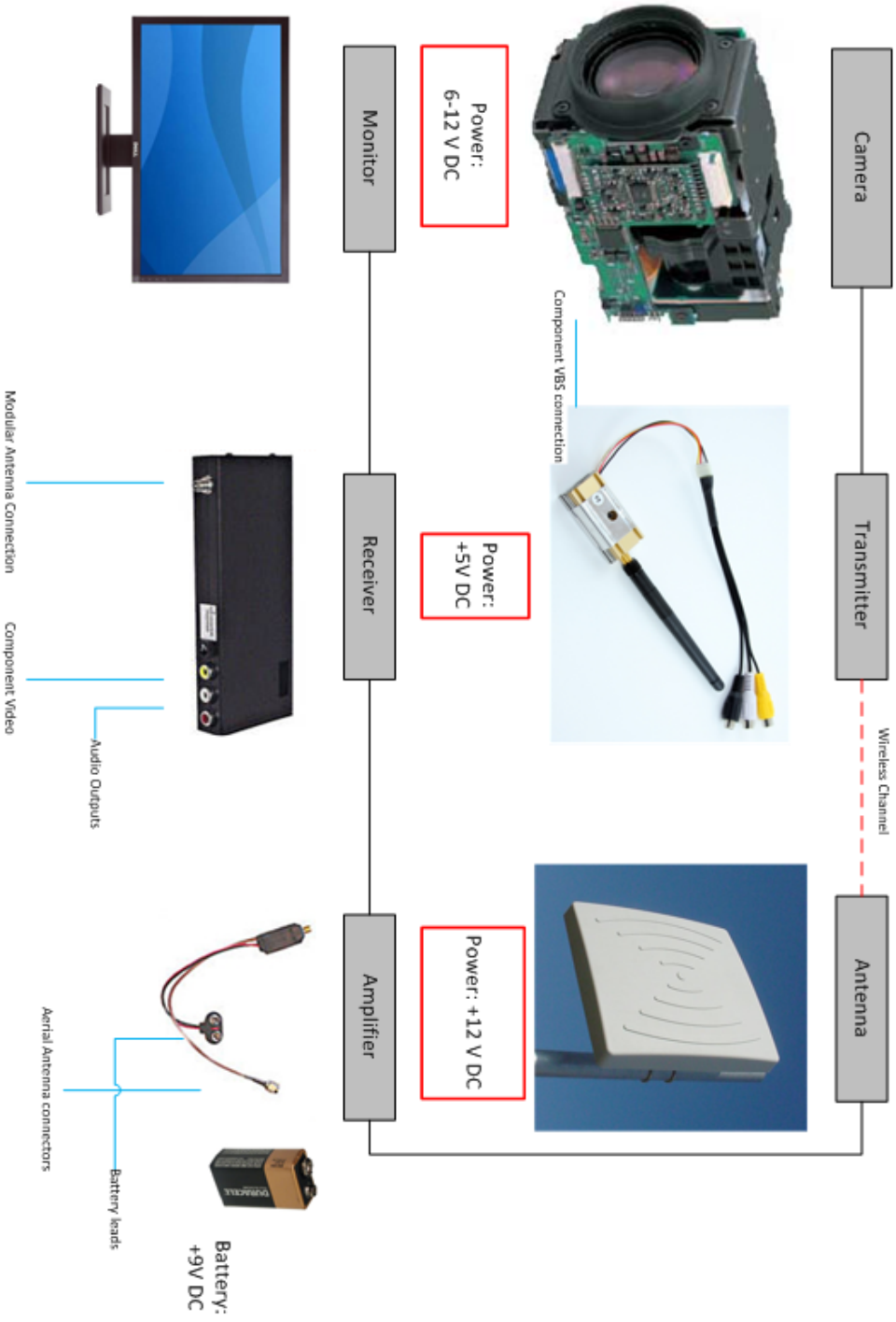

B.2 Power Supply System Detail